UC San Diego

UC San Diego Electronic Theses and Dissertations

Title

Receiver designs for multiuser underwater acoustic communications

Permalink

https://escholarship.org/uc/item/9fw5x6ww

Author

Cho, Steve E.

Publication Date

2012

Peer reviewed|Thesis/dissertation

eScholarship.org Powered by the California Digital Library
University of California

UNIVERSITY OF CALIFORNIA, SAN DIEGO

Receiver Designs for Multiuser Underwater Acoustic Communications

A dissertation submitted in partial satisfaction of the
requirements for the degree
Doctor of Philosophy

in

Electrical Engineering
(Communication Theory and Systems)

by

Steve E. Cho

Committee in charge:

William S. Hodgkiss, Chair
Bhaskar D. Rao, Co-Chair
Ryan Kastner
William A. Kuperman
John G. Proakis
Hee Chun Song

2012

Copyright
Steve E. Cho, 2012
All rights reserved.

The dissertation of Steve E. Cho is approved, and it is acceptable in quality and form for publication on microfilm and electronically:

_____

_____

_____

_____

_____
Co-Chair

_____
Chair

University of California, San Diego

2012

TABLE OF CONTENTS

LIST OF FIGURES

LIST OF TABLES

ACKNOWLEDGEMENTS

I would like to acknowledge my advisors, Bill Hodgkiss and Heechun Song, for their patience, guidance, and support through all of my academic endeavors.

I would also like to thank my committee Co-Chair, Bhaskar Rao, and the rest of the committee, for their guidance and support.

This work would not have been possible without the hard work of those at Marine Physical Laboratory and other institutions who contributed to the at-sea experiments that were pivotal to this work.

Finally, I would like to acknowledge my friends and family, whose never ending support has guided me over the years.

Chapter 2, in full, is a reprint of the material as it appears in "Successive Interference Cancellation for Underwater Acoustic Communications, S. E. Cho, H. C. Song, and W. S. Hodgkiss, *IEEE Journal of Oceanic Engineering*, Vol. 36, No. 4, August 2011, pp. 490–501. The dissertation author was the primary investigator and author of this paper.

Chapter 3, in full, is a reprint of the material as it appears in "Multiuser Interference Cancellation in Time-Varying Channels, S. E. Cho, H. C. Song, and W. S. Hodgkiss, *Journal of the Acoustical Society of America*, Vol. 131, No. 2, January 2012, pp. EL163–EL169. The dissertation author was the primary investigator and author of this paper.

Chapter 4, in full, is a reprint of the material as it appears in "Asynchronous Multiuser Underwater Acoustic Communications, S. E. Cho, H. C. Song, and W. S. Hodgkiss, *Journal of the Acoustical Society of America*, in press, 2012. The dissertation author was the primary investigator and author of this paper.

Chapter 5, in full, is a reprint of the material as it appears in "Multiuser Acoustic Communications with Mobile Users, S. E. Cho, H. C. Song, and W. S. Hodgkiss, *Journal of the Acoustical Society of America*, submitted on May 29, 2012. The dissertation author was the primary investigator and author of this paper.

VITA

2007	B. S. in Electrical Engineering, The University of Texas at Austin
2008–2012	Graduate Research Assistant, University of California, San Diego
2009	M. S. in Electrical Engineering (Communication Theory and Systems), University of California, San Diego
2012	Ph. D. in Electrical Engineering (Communication Theory and Systems), University of California, San Diego

PUBLICATIONS

S.E. Cho, H.C. Song, W.S. Hodgkiss, "Successive Interference Cancellation for Underwater Acoustic Communications", *IEEE Journal of Oceanic Engineering*, Vol. 36, No. 4, pp. 490–501, 2011.

S.E. Cho, H.C. Song, W.S. Hodgkiss, "Multiuser Interference Cancellation in Time-Varying Channels", *Journal of the Acoustical Society of America*, Vol. 131, No. 2, pp. EL163–EL169, 2012.

S.E. Cho, H.C. Song, W.S. Hodgkiss, "Asynchronous Multiuser Underwater Acoustic Communications", *Journal of the Acoustical Society of America*, in press, 2012.

S.E. Cho, H.C. Song, W.S. Hodgkiss, "Multiuser Acoustic Communications with Mobile Users", *Journal of the Acoustical Society of America*, submitted, 2012.

ABSTRACT OF THE DISSERTATION

Receiver Designs for Multiuser Underwater Acoustic Communications

by

Steve E. Cho

Doctor of Philosophy in Electrical Engineering
(Communication Theory and Systems)

University of California, San Diego, 2012

William S. Hodgkiss, Chair
Bhaskar D. Rao, Co-Chair

This dissertation focuses on multiuser communications through shallow, underwater acoustic channels. These channels are characterized by channel impulse responses with long delay spreads undergoing rapid fluctuations with respect to the digital signaling time. When multiple users (e.g. AUVs, gliders, or sensor nodes) need to transmit information to a common receiver, they must share the channel in some fashion. The designs presented in this dissertation utilize a sharing scheme known as Space Division Multiple Access (SDMA), where the inherent disparity in the impulse responses sampled at different spatial locations are leveraged by the system to provide users with interference-free uplinks to the common

receiver. Compared to other channel sharing methods, SDMA benefits from high data throughput and a low reliance on feedback from the receiver, two desirable qualities in a bandwidth limited, rapidly evolving environment.

The receivers discussed throughout this dissertation will employ successive decoding techniques to retrieve each user's information independently but will use knowledge from previous decoding cycles to model and remove multiple access interference along the way. With multiple iterations of estimation and interference cancellation, these receivers will progress towards the goal of providing each and all of the users with interference-free uplinks to the receiver. Three receivers will be discussed in this dissertation with each successive design more generally applicable than the previous: one will be applicable in time-invariant environments between geographically fixed users and a fixed, multiple-element receiver, the next will be applicable in a time-varying environment between fixed users and a fixed receiver array, and the final design will be applicable in situations with users in motion. All of the receivers discussed will require direct knowledge of the impulse response and will employ sparse channel estimation techniques to acquire this information and track any changes while decoding. The capabilities of all of the receivers will be analyzed with data collected during at-sea experiments.

Chapter 1

Introduction

This dissertation discusses the problem of multiuser underwater acoustic communications (UWAC). In underwater environments, microwave transmissions (roughly from 1 GHz to 30 GHz) typically used in over-the-air wireless communications (e.g. television, cellular, and wireless local area networks) experience severe attenuation at ranges of just a few meters and typically are not appropriate for wireless underwater communications. Furthermore, electromagnetic radiation at optical wavelengths are useful for communications only up to about a hundred meters [3]. At ranges of a hundred meters to a few kilometers, communications signals instead are transmitted acoustically (from roughly 1 kHz to 100 kHz) where the attenuation is much less severe. In fact, acoustic communications at even lower frequencies (tens to hundreds of Hz) have been explored at ranges from a few hundred up to a few thousand kilometers [4, 5]. Communications at these low frequencies constrain strictly the useful portion of the frequency band, known as the available bandwidth, to be quite small in relation to wireless channels, limiting the total possible amount of information that can be communicated successfully. Thus, recent advances in UWAC, whether single or multiuser, have been focused on bandwidth efficient designs including high-order constellations, multi-carrier signals, and multiple transmit/receive antennas, among others [6].

Of particular interest to this dissertation is the problem of multiuser communications, or scenarios when multiple sources of information are present. For example, one can imagine a small number of autonomous undersea vehicles (AUVs),

gliders, or data sensors, that wish to transmit either their location, observed data, or perhaps some other information to a common base station in a wireless fashion. If the goal of the base station is to receive and decode the information from all of the sources, referred to as the users of the channel, the UWAC system must be designed to allow them to share the resources of the communications channel. For example, the users could transmit during non-overlapping time slots or over non-overlapping portions of the available bandwidth, reducing their individual throughput in exchange for minimizing or eliminating multiple-access interference (MAI) from the other users. Indeed, almost all modern wireless systems are designed around these exact principles, some of which will be discussed in the following sections. However, not all candidate solutions to this design problem are the same, and the study and comparison of these is broadly known as multiuser or multiple-access communications (MAC).

Before an overview of modern MAC systems, a familiarity with the shallow underwater acoustic channel will be necessary, since the constraints imposed by this environment will impact the choice of MAC deigns. A short review of MAC system designs will follow with remarks on their specific applicability to the underwater acoustic channel. A few candidate multiuser receiver architectures will then be discussed that are designed for multiple-access systems in shallow underwater acoustic channels.

1.1 Shallow Underwater Acoustic Channels

Underwater acoustic channels have many characteristics that are unique to typical wireless channels, namely the impact of the dynamics of the ocean, geometry of the source and receiver, among others [7]. However, there are a few that have particularly important consequences when it comes to MAC systems that will be discussed in the following sections.

1.1.1 Multipath Arrivals

One of the main characteristics of the shallow water channel is the presence of two lossy reflectors: the sea surface and the sea floor. Fig. 1.1 is a simplified illustration of the impact of these reflectors on acoustic propagation from an omnidirectional source in a homogenous medium. Of course, the ocean is not a homogenous medium and the sea surface and sea floor are far from smooth reflectors, and accurate modeling of acoustic propagation requires much more detailed analysis [8]. However, the simple illustration in Fig. 1.1 does provide some general intuition. In the absence of reflectors, the received signal contains only one copy of the transmitted waveform, in this case a Dirac delta function $\delta(t)$, observed after a propagation delay (i.e. the ratio of the distance traveled to the speed of the wave). With one lossy reflector, the received signal contains the same direct path arrival as if there were no reflector, but also contains another copy of $\delta(t)$ at a later point in time. This "1-bounce" path arrives later than the direct path because it must travel a longer distance before reaching the receiver. Also, because the reflector is lossy, some of its energy is lost when this wave is reflected. Finally, with two lossy reflectors, a large number of arrivals are possible (only 3 are shown in Fig. 1.1). Each path is observed at the receiver at an arrival time determined by the path length and the speed of the wave in the medium. To describe succinctly the structure of the multipath arrivals, the superimposed, delayed copies of a transmission of $\delta(t)$, a function known as the channel impulse response (CIR) is defined. The CIRs in the previous simplified illustration are displayed in the lower panels of Fig. 1.1.

An important consequence of this resolvable multipath is the large delay spread of the CIR which can cause significant intersymbol interference (ISI) at the receiver. The delay spread is defined as the time separation between the first and last arrivals (i.e. the non-zero span or support of the CIR), which is simply calculated as $\Delta d/c$, where Δd is the difference in path lengths, and c is the speed of wave propagation in the medium. In wireless communications, electromagnetic waves transmitted through the air travel close to the speed of light ($c \approx 3 \times 10^8$ m/s), and the delay spread tends to be no more than a few

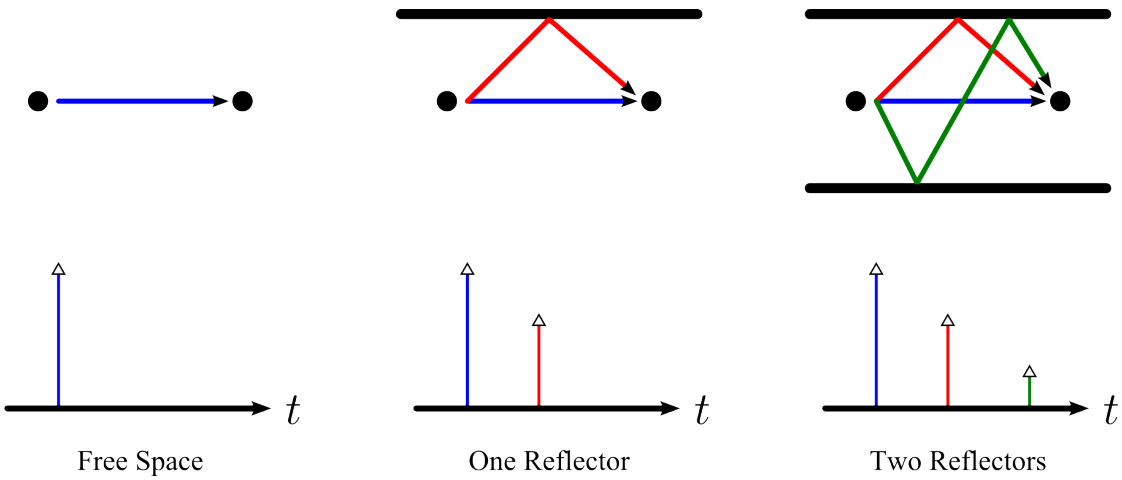

Figure 1.1: Comparison of propagation in free space (left), in the presence of one lossy reflector (middle), and between two lossy reflectors (right). The geometry of the source and receiver support a discrete number of possible propagation paths. The bottom panels illustrate the channel impulse responses for each geometry which capture both the amplitude and timing of the arrivals at the receiver.

symbol periods. However, in underwater acoustics, wave propagation is restricted to the slow speed of sound in the ocean ($c \approx 1500$ m/s) which causes the delay spread to span tens or potentially hundreds of symbol periods and can introduce severe ISI.

An example CIR from an ocean environment is presented in Fig. 1.2. This CIR was observed in at-sea trials conducted during the Kauai Acomms MURI 2011 (KAM11) experiment, from which data were used for this dissertation. A source at a depth of 76 m transmitted over the 20-30 kHz bandwidth, and the CIR between the source and the ith receiver element, denoted $h_i(t)$, was observed across the entire array. This trial was conducted in 100-m deep water over a range of approximately 3 km. For this example, symbols were transmitted every 0.2 ms, suggesting the delay spread of 10 ms would lead to ISI of 50 symbol periods for this system. This severity of ISI is common in UWAC and requires careful consideration in system designs.

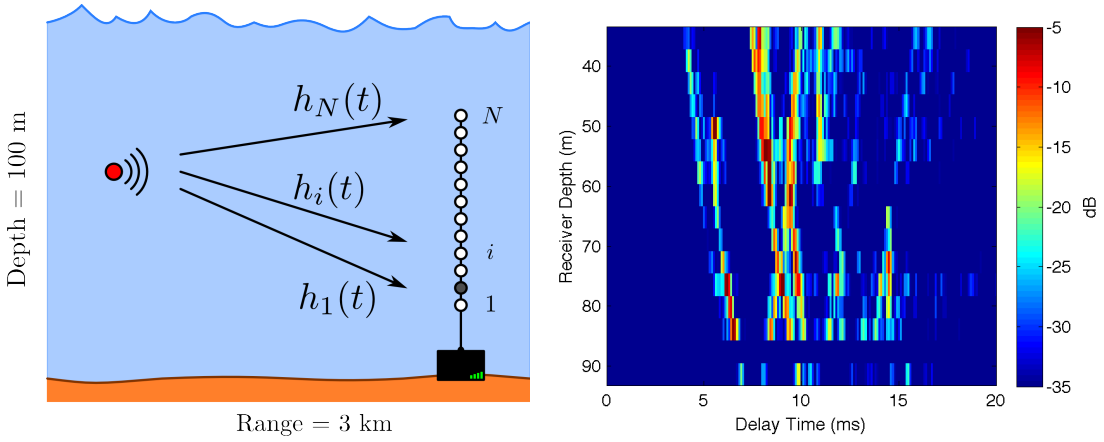

(a) (b)

Figure 1.2: (a) Diagram of the KAM11 experiment conducted in 100-m deep water with one source and a 16-element receiving array at 3 km range, and (b) intensity of CIRs measured at 15 of the array elements. Data from a malfunctioning element at 87-m depth were excluded.

1.1.2 Time-Varying Channels

The physical properties of the ocean are always changing, from endless undulations of the sea surface that alter the reflection pattern of incident rays to internal tides and currents altering the speed of sound. These changes, among many others, manifest themselves in CIRs that also undergo rapid changes, requiring systems to adapt to their temporal instability during processing. As an example of such dynamics, the left panel of Fig. 1.3 illustrates the evolution of the CIR observed at the deepest element (91-m depth) from Fig. 1.2 over a typical packet length.

The time-scale of variations can be characterized by the coherence time of the channel, a measure of how relevant or coherent a snapshot of the CIR at any point in time is likely to be in the future. Formally, the coherence time is defined as the inverse of the coherence bandwidth, a measure of the severity of Doppler spread in the channel [9]. In UWAC, CIRs can change very rapidly, and coherence times tend to be very small and may only be tens of milliseconds. Small coher-

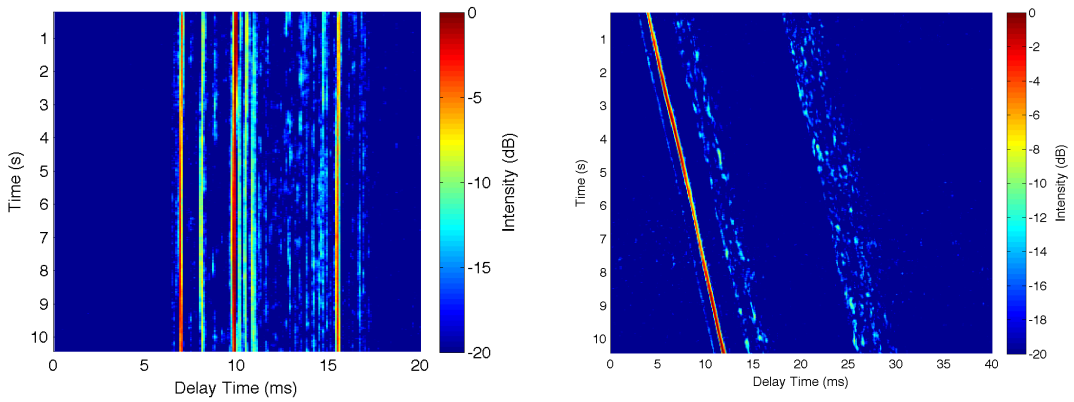

Figure 1.3: Time-varying CIRs from the KAM11 experiment observed at the deepest element (91-m depth) of the receiving array from a stationary source (left) and a source moving away from the receiver at 1.5 m/s (right).

ence times are especially consequential when coupled with the long propagation time due to the slow speed of acoustic waves in UWAC. With a speed of sound in water of around 1500 m/s, transmissions between the source and receiver may take a few seconds to travel through the ocean and arrive at their destination. By the time the receiver has decoded the packet, measured the CIR, and relayed this channel information to the source, many seconds will have passed likely surpassing the coherence time of the channel, and the receiver's measurement of the CIR will likely no longer be relevant. In terms of multiple-access systems, the impact of large travel times and small coherence times is the severe limitation of the feedback channel, the communications channel from the receiver back to the user(s), which is heavily used in the over-the-air wireless channel to schedule users, relay channel information, and request changes to the transmissions (transmission power, modulation, etc.) to best serve the overall system. As will be discussed in the following sections, underwater MAC systems that do not rely heavily on the feedback channel will be desirable for this very reason.

The speed of these variations are exacerbated when the source or the receiver is in motion, as shown in the right panel of Fig. 1.3. This time-varying CIR was estimated during KAM11 from a communications packet over a span of 10.5

seconds while the user was traveling at 1.3 m/s away from a stationary receiver at an initial range of approximately 1.3 km. There are two main differences when comparing the CIR from the moving source to that of the stationary source in the left panel of Fig. 1.3. First, the multipath arrivals appear to drift in arrival time. With the source traveling away from the stationary receiver, the path lengths increase slowly over time, increasing the travel time with each successive measurement of the CIR. Second, the paths appear to fade in and out at a faster rate, especially the weaker, multiple bounce paths, in comparison to the CIR measured from the stationary source. Even when the drift in arrival times can be corrected through a resampling process, the rapid fades in the arrivals must still be tracked accurately by the receiver.

The effect of source or receiver motion in UWAC is non-trivial, and is discussed in further detail later in this dissertation.

1.2 Survey of Multiple-Access Systems

With some of the important characteristics of the underwater acoustic channel in mind, our focus turns to multiple access system designs. When multiple users need to transmit their information to a shared base station, the communications channel must also be shared. Like a consumable resource, the channel is divided in some fashion, with each user consuming one piece of the total channel. How the division is performed is the central design problem, and the properties of the shallow water acoustic channel will impact greatly the choice of a particular division scheme. Below, some popular candidates are reviewed, and comments on their possible applications to multiuser UWAC are provided.

1.2.1 Time Division Multiple Access

Time Division Multiple Access (TDMA) is a simple division scheme in terms of design complexity. Depicted in Fig. 1.4, TDMA assigns to each user time slots for packet based transmission. During their designated time sots, users transmit packets occupying the entire available bandwidth $[f_c - W/2, f_c + W/2]$.

Multiple-access interference (MAI), the interference from other users in the system, is eliminated by ensuring no two users transmit during identical time slots. Guard intervals typically are included between time slots to ensure the large multipath delay does not introduce MAI. As noted in the UWAC literature [10], the main disadvantage of TDMA is that it requires strict synchronization amongst the users. The system must be designed to ensure that all users transmissions are separated in time at the receiver, which could be achieved with a periodic probe transmission from the receiver to allow the users to compensate for their differences in propagation delays. However, another disadvantage of TDMA is the throughput cost necessary to prevent MAI in this manner. When one user is transmitting, all others must remain silent, and thus, the total system throughput will never exceed that of a single user occupying the entire channel at all times.

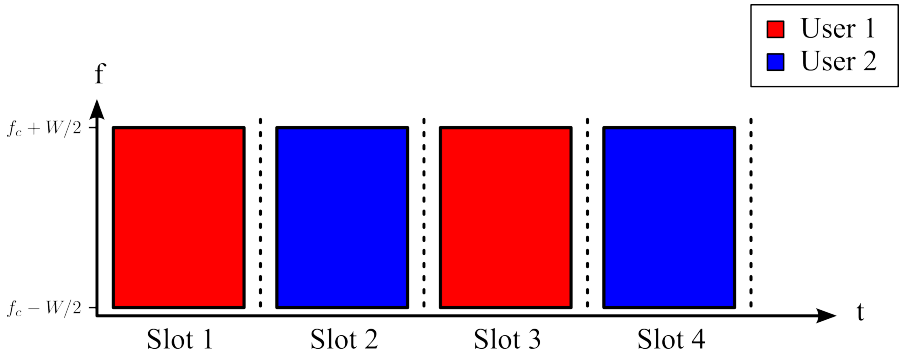

Figure 1.4: Diagram of TDMA for a system with two users. Each user is assigned time slots for transmission. Strict synchronization is required for the system to avoid MAI.

1.2.2 Frequency Division Multiple Access

Frequency Division Multiple Access (FDMA) is another simple division scheme that instead divides the available bandwidth into smaller bands to be occupied by each user as depicted in Fig. 1.5. MAI is prevented by ensuring no two users occupy the same frequency band. The strict synchronization requirement of TDMA is not an issue for FDMA, since all users can transmit simultaneously with this scheme. However, a feedback channel still is necessary to assign to each

user one of the available bands. Another downside of FDMA is that it also suffers the same throughput restriction of TDMA. Each user occupies only a small portion of the bandwidth, and thus must reduce their individual throughput to ensure MAI prevention for the system as a whole. The total system throughput with FDMA will never exceed the throughput achieved by a single user occupying all of the frequency bands at all times.

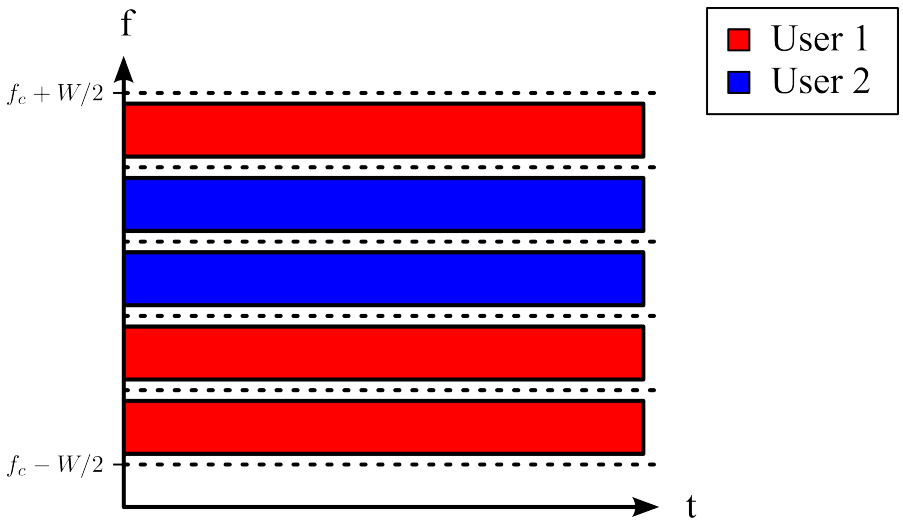

Figure 1.5: Diagram of FDMA for a system with two users. Each user is assigned frequency bands for transmission. Users must occupy only their assigned bands to avoid MAI.

1.2.3 Code Division Multiple Access

Compared to TDMA and FDMA, Code Division Multiple Access (CDMA) is a slightly more complicated design, but can be implemented by the users and the receiver in a simple fashion. In CDMA, each user constructs a narrowband signal for transmission. Then, the users spread their narrowband signal to cover the available bandwidth through convolution with predetermined spreading codes unique to each user. At the receiver, a single user's signal can be isolated by de-spreading the combined signal with the user's spreading code. The de-spreading operation suppresses both MAI from other users as well as any narrowband noise sources. Because CDMA techniques spread narrowband signals over the available

bandwidth, CDMA techniques are among the more general category of spread spectrum communications, where single and multiuser communications research efforts have taken place [11, 12, 13, 14].

The key to CDMA is the proper construction of the set of spreading codes used by the users. Popular choices (e.g. Kasami codes and Gold codes) can be constructed easily at various spreading gains from maximal-length pseudo random sequences and can provide some guarantees on the severity of residual MAI after de-spreading [9]. An example Kasami code set for a system of four users is shown in Fig. 1.6. The most important characteristic of all spreading codes is the number of chips, also known as the spreading gain (15 in Fig. 1.6). As the spreading gain increases, so does the MAI suppressive capability of the system. However, the spreading gain cannot be increased arbitrarily. Assuming the total available bandwidth is fixed, increasing the spreading gain decreases linearly the throughput of each user, and a tradeoff between data rate and MAI suppression must be considered.

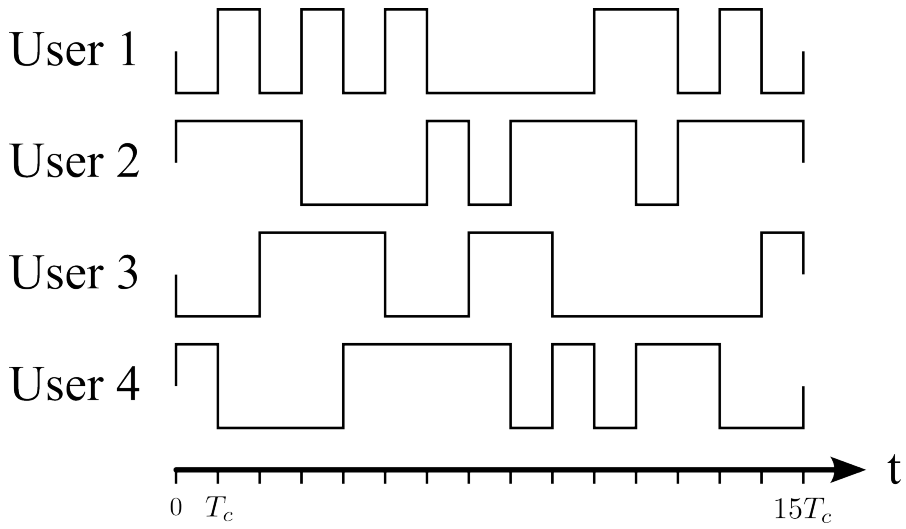

Figure 1.6: Diagram of a Kasami codebook for a CDMA system supporting a maximum of four users. With this codebook, each user transmits a symbol every $15T_c$ seconds where T_c is the chip interval. The receiver de-spreads using the same codebook to suppress MAI.

One of the strengths of CDMA for multiple-access systems is that it does

not require synchronization of any kind between the users. Any user can begin or end transmissions at any time, eliminating or reducing greatly the scheduling overhead needed in other multiple-access schemes (e.g. TDMA). Thus, the need for a feedback channel is minimized greatly with CDMA, making it a popular choice for underwater MAC [15, 16].

1.2.4 Space Division Multiple Access

Space Division Multiple Access (SDMA) is a multiuser division scheme that relies on the spatial separation between the users and the different channel responses they may experience due to the complexities of the channel to separate them at the receiver. Much like a multiple-antenna receiver observes a different interference pattern at each of its spatially separated antennas, the CIRs from users that are separated in space may also appear distinct when observed at the receiver. These differences can be used to achieve array gains and antenna diversity in multiple-antenna receivers, and in the case of multiple separated transmitters (i.e. users), the differences can be used to achieve spatial diversity.

As an example, Fig. 1.7 illustrates the CIRs estimated from two spatially separated users at each of 16 elements in a vertical array from the KAM11 experiment. The users were separated vertically by 15 m while transmitting over a range of 3 km to the receiver. Fig 1.7 illustrates only a snapshot the time-varying CIRs, which evolved through time and had to be tracked by the receiver. However, the differences in these channel responses, if properly estimated and tracked at the receiver, could be used potentially to separate the their signals and to decode their transmissions with a low probability of error.

Similar to CDMA systems, the received signal in SDMA contains components that are different and can be used to identify each user (e.g. unique spreading codes in CDMA, and unique CIRs in SDMA). In the case of CDMA, the uniqueness built into the signal comes at the cost of throughput, since the bandwidth of the data-bearing signal must be reduced as the spreading gain (and the capability to suppress MAI) is increased. In SDMA, the uniqueness is not built into the transmitted signal and is instead provided by the channel. This

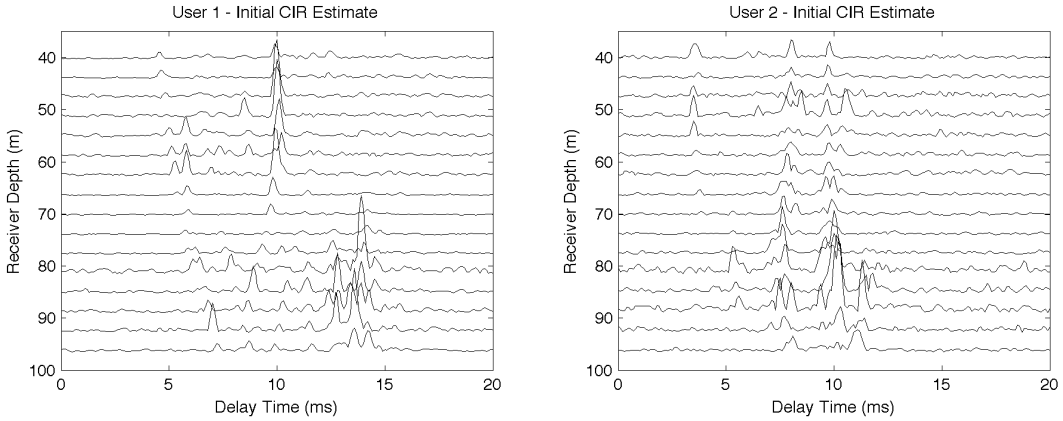

Figure 1.7: Illustration of CIRs from each of two users separated by 15 m to a 16 element receiving array at a range of 3 km. In SDMA, the differences in these CIRs are used to separate the user transmissions at the receiver.

has two important implications. First, the users may transmit wideband signals instead of narrowband signals, achieving potentially higher throughputs than may be possible in CDMA designs. Second, while the spreading codes in CDMA can be designed to be very nearly orthogonal, reducing greatly the amount of MAI after de-spreading, SDMA provides no such guarantees. Consequently, receiver designs in SDMA must deal with the strong MAI at the receiver and typically are more complicated than CDMA receivers. However, much like CDMA systems, the feedback channel is not heavily relied on in SDMA designs since the users may occupy the entire bandwidth and may initiate their transmissions at any time, reducing the need for synchronization between themselves and between themselves and the receiver.

The focus of this dissertation will be SDMA systems. Receiver designs will be presented that can achieve the same goal common to all MAC designs, i.e. providing each user with an interference free channel, but without the need to sacrifice throughput.

1.3 Recent Work

Compared to single user UWAC, multiuser communications is a relatively unexplored area of research. Most of the existing research utilizes CDMA based designs, assigning to each user a predetermined code to spread their narrowband signal over the available bandwidth. There are, however, notable exceptions, namely some recent research efforts that have yielded receiver designs based on SDMA. These recent advances can broadly be fit into two categories: those employing exclusively multichannel adaptive equalizers and those employing time-reversal combiners. These two types of multiuser receivers will be introduced in the following sections.

1.3.1 Adaptive Decision-Feedback Equalizers

Adaptive decision-feedback equalizers (DFEs) were the basis for some of the first receiver designs for phase coherent underwater acoustic communications [17, 18]. These DFEs embedded a phase-locked loop between the equalizer feedforward and feedback filters to combat the rapid phase fluctuations in UWAC. The early versions of this work updated the coefficients of the feedforward and feedback filters jointly to minimize the error at the input to the symbol decision device. Another interesting examination produced a version of the equalizer employing direct knowledge of the CIR to reduce the computational complexity and to improve the performance of equalizer [19]. A further investigation extended this work to multiuser communications, employing both a single equalizer to decode all of the users' messages jointly, as well as a suboptimal approach that would decoded them with independent equalizers [1].

Although the joint multiuser DFE was derived to decode optimally the users' information in the mean-squared error sense, this particular equalizer lacked somewhat in practicality. The major drawback of the optimal joint DFE was its need to track and adapt the filter weights for all of the users simultaneously. In UWAC, adaptive DFEs require a large number of taps even in single user systems because of the large delay spread of the channel, and with the addition of multiple

users, the computational complexity involved in tracking all of the taps together made this optimal receiver infeasible. Although a suboptimal version was discussed in [1], this version did not explicitly track or remove MAI to aid in the decoding process.

Adaptive DFEs will be discussed further throughout the remainder of this dissertation.

1.3.2 Time-Reversal Combiners

Time-reversal (TR) processors have become a popular alternative to adaptive DFEs for phase coherent communications in underwater acoustic channels. In contrast to most adaptive DFEs (with the exception being the channel estimate directed version), TR processors apply directly their estimates of the channel as time domain filters. TR processing is also commonly referred to as phase conjugation and can be applied in two ways. First, active TR (or active phase conjugation) utilizes channel estimates at the transmitter in a pre-filtering operation. This is done so that the distortion caused by the channel in fact applies the phase conjugated version of the filter, focusing the signal at the receiver. This process invokes the reciprocity of the underwater acoustic channel, but requires time-invariance in the CIRs to be effective.

More commonly, passive time-reversal (or passive phase conjugation) is applied at the receiver. In this version, the receiver applies estimates of the channel as a temporal matched filter. That is, the received signal from each channel is filtered with the time-reversed version of the CIR measured at that channel, and the outputs from all channels are coherently summed before further processing [20, 13]. The result is a single-channel output with an effective channel known as the q-function. With enough properly spaced receiver elements, the q-function closely resembles a Dirac delta function $\delta(t)$, allowing the receiver to employ much simpler processing on the output of the TR combiner. However, since direct knowledge of the channel is required, frequent adaptation may be necessary to track the temporal variations of the channel [21].

Interestingly, with multiple transmitters, passive TR combiners can be used

to isolate one of the transmitters, suppressing (but not eliminating) the interference from the others. When the transmitters cooperate to transmit a single stream of information, this is known as multiple-input, multiple-output communications [22]. When the transmitters act independently, it is multiple-access or multiuser communications [23, 2, 24]. The suppressive capability of the combiner in either scenario depends wholly on the characteristics of the CIRs between each transmitter and each receiver element. If the CIRs from all pairs of users are orthogonal at every receiver, then the conventional TR combiner can separate the users without residual interference. However, this hardly is the case, and in reality some interference mitigation is required. Adaptive TR combiners are capable of suppressing MAI [25], but previously have not been applied with multiple users in time-varying channels. Some recent work on MAI removal for TR combiners includes a parallel interference cancellation technique which decodes the users jointly with MAI removed along the way [24].

Passive TR combiners, both conventional and adaptive, will be discussed in detail in the remaining chapters. Specifically, the effects and eventual removal of MAI when employing these processors in underwater acoustic environments will be the central focus of this dissertation.

1.4 Preview of Remaining Chapters

The remainder of this dissertation will be organized as follows.

Chapter 2 will discuss MAC in time-invariant underwater acoustic environments. A multiuser receiver will be formed by embedding a conventional TR processor within the SIC framework. Because the receiver has full knowledge of the time-invariant CIR between each user and each receiver element, interference estimates will be formed by combining previously decoded symbols with the cross q-functions determined by the complete set of CIRs. This receiver will be applied in an iterative fashion to at-sea experimental data collected during the FAF-05 and FAF-06 experiments and compared to a DFE-based multiuser receiver.

Chapter 3 will discuss MAC in time-varying environments restricted to sta-

tionary sources and receivers. This receiver applies three important modifications to the previous architecture. First, interference cancellation is performed at the multichannel level to mitigate MAI in preparation of channel updates. Second, the MP algorithm will be employed to produce sparse channel estimates to adapt the receiver as the channel fluctuates. Finally, adaptive time-reversal (ATR) will be introduced to provide additional MAI mitigation as well as suppression of error propagation in the feedback portion of the receiver. This receiver also will be applied in an iterative fashion to at-sea experimental data collected during the KAM11 shallow water experiment.

Chapter 4 will discuss asynchronous multiple-access communications. The previous chapter discussed the applicability of the joint SIC, ATR, and MP in time-varying ocean environments, but did not discuss the initial acquisition of CIR required by all TR receivers. Unlike single-user TR receivers, multiuser TR receivers in general must estimate the initial CIR from each user in the presence of strong MAI. This chapter illustrates that in the absence of a feedback channel when users generally transmit in an asynchronous fashion, their initial CIR can be estimated and their packets decoded successfully with the SIC, ATR, and MP receiver. This chapter also provides data examples from the KAM11 shallow water experiment.

Chapter 5 discusses MAC in time-varying environments without the restriction of stationary sources. When any or all of the users are allowed to communicate while in motion, the receiver must compensate for the Doppler effect. The receiver discussed in this chapter modifies the joint SIC, ATR, and MP receiver to both retrieve a desired user's signal at a Doppler frequency shift, but to also mitigate interference from sources at potentially different Doppler frequency shifts. This chapter will also discuss data collected from the KAM11 experiment but with a source in motion.

Chapter 6 will summarize the dissertation and discuss possible avenues for future research.

Chapter 2

Successive Interference Cancellation for Underwater Acoustic Communications

In this paper, we introduce the addition of an iterative, successive interference cancellation (SIC) process to improve on a multiuser, single-input/multiple-output communications receiver using passive time-reversal as a space-time preprocessor. Time-reversal has been shown to apply the spatial degrees of freedom to enhance the signal-to-noise ratio (SNR) and suppress interference for a target user. With the introduction of SIC, the receiver can remove the residual interference experienced by each user while preserving the SNR gain achieved by time-reversal prepocessing. The SIC process is a decision-directed approach for removing multiuser interference at the receiver and is similar to the decision-directed, feedback equalizer (DFE) for intersymbol interference channels. The interference experienced by each user is estimated at the receiver using previously decoded symbols from interfering users. This estimate is scaled and synchronized before subtraction from the target user's signal after time-reversal combining. Since SIC is applied prior to symbol decoding, symbol estimates are improved as the process is allowed to iterate until a stationary point is reached. Following time-reversal combining and SIC, a DFE can mitigate any remaining intersymbol interference before symbol decisions are made. Data collected from two experiments (FAF-05 and FAF-06)

are used to demonstrate the performance of the proposed interference cancellation scheme. During the FAF-05 experiment, 3 users transmitted 16-QAM symbols simultaneously over the 3-4 kHz frequency band to a 20-element receiving array deployed in 120-m deep water at a range of 20 km. The FAF-06 experiment included the simultaneous transmissions of 8-QAM symbols from 2 users over the 9-21 kHz band to a 16-element receiving array in 92-m deep water at a range of 2.2 km. For both of the examples, SIC is shown to improve the output SNR in the presence of strong interference over time-reversal processing alone. This translates to a significant bit-error rate reduction from 1.53×10^{-2} to 8.80×10^{-4} for the FAF-05 data and from 1.77×10^{-3} to error-free decoding for the FAF-06 data.

2.1 Introduction

Point-to-point communications through the underwater acoustic channel has been extensively studied since the feasibility of a phase-coherent receiver was demonstrated in [17], with its extension to a multichannel receiving array in [18]. It is well known that receiving arrays can enhance the signal-to-noise ratio (SNR) of a communications link by coherently combining multiple receptions of a single transmission. Ideally, if the channel to each receiving element is spatially uncorrelated, then each element can provide an additional spatial degree of freedom for decoding the transmission. However, the addition of multiple transmitters can exploit the channel differently, i.e. by utilizing the expanded spatial diversity to instead create parallel channels for simultaneous transmission of independent information streams from a single or multiple users. The potential effect of the latter is a linear increase in capacity, whereas the former can only provide a logarithmic increase in capacity.

Recently, these properties have been applied to point-to-point communications in the form of multiple-input/multiple-output (MIMO) system designs [26], which have demonstrated significant throughput gains in shallow water environments. A particular instance of the MIMO channel is the multiuser single-input/multiple-output (SIMO) channel, in which multiple users send their mes-

sages to the receiving array each using a single transmitter (e.g., see Fig. 2.3). This multiple access model is of particular interest to the underwater uplink channel, in which acoustic transmissions are typically sent by a small number of power-limited devices with single transducers (sensors, AUVs, gliders, etc.) to a receiving base station with multiple receiving elements and abundant processing capabilities.

However, the broad description of the multiuser SIMO model does not sufficiently characterize the multiple-access underwater acoustic communications channel. An intelligent design must also consider factors such as limited bandwidths, large delay spreads, and long propagation delays. For example, the severe bandwidth limitations of the underwater acoustic channel force all users to transmit over the entire band to achieve higher data rates. In addition, multiuser interference can be severe due to the large delay spreads in underwater settings. Furthermore, long propagation delays penalize heavily feedback-dependent communications schemes. These factors motivate a limited-feedback communication design in which multiple users are able to access the channel simultaneously and over the same frequency band.

Joint decoding of superimposed multiuser transmissions has been extensively studied for wireless channels over the last 20 years [27] in which small delay spreads and block-fading assumptions have led to near-optimal receiver designs with light computational complexity. Applications to the underwater acoustic channel, in which these assumptions must be relaxed, previously have led to computationally-heavy, adaptive receivers designed to compensate simultaneously for both the dispersive channel and multiuser interference [1]. In this previous work, the optimal multiuser detector was derived to jointly minimize the mean-squared error of all symbols transmitted through the system, achieving simultaneous decoding of all users. However, this system was deemed overly complex, and a suboptimal version was presented that separated the problems of spatial combining and multichannel equalization and detected each user in parallel (without symbol information from competing users) achieving a significant complexity reduction.

The objective of this paper is the study of a multiuser receiver that again separates the problems of spatio-temporal combining and equalization. However,

the proposed architecture decodes the users in succession, estimating and removing interference from previously decoded users in the process. This concept of successive detection of multiuser signals is certainly not new, this family of receivers has become a popular choice for multiuser detection in the wireless community [27]. The basic structure of the proposed multiuser detector is comprised of three components. First, a time-reversal combiner [23], designed to focus the receiving array on a particular user in space and time, is employed to create parallel (but not necessarily independent) channels for each user while suppressing intersymbol interference (ISI). Receiver architectures with passive time-reversal preprocessing have been shown to simplify overall system designs while maintaining near-optimal performance [28, 29]. Second, following passive time-reversal, an interference cancellation scheme processes previously decoded messages from all competing users to negate multiuser interference for a target user. Upon successful cancellation of interference for all users, the multiuser SIMO channel is transformed into an ensemble of independent, single-input/single-output (SISO) communication channels degraded solely by residual ISI from time-reversal processing. Third, a decision-feedback equalizer (DFE) compensates for the remaining ISI before symbol decisions are made. It should be mentioned that an alternative formulation for multichannel combining with additional interference mitigation using adaptive, passive time-reversal also has proven to be successful [25].

Before deriving the structure of the proposed multiuser receiver, a sufficient time-invariant model for the underwater acoustic channel is developed in Section II. Then, the iterative Successive Interference Cancellation (SIC) receiver is described in Section III. In Section IV, the receiver is applied to experimental data from the Focused Acoustic Fields experiments conducted in both 2005 (FAF-05) and 2006 (FAF-06).

2.2 System Model

Accurate modeling of the underwater acoustic channel is still a challenging problem. For the purposes of this paper, we need only to derive a measurable

quantity that can characterize sufficiently the performance of successive interference cancellation over channels after time-reversal combining. First, the channel model is derived between a single transmitter and a receiver array. Then, the model is expanded to support multiple users. Finally, passive time-reversal is described, and multiuser interference is characterized within this context. For the remainder of this paper, $*$ will denote the convolution operator while $\dagger$ will denote a complex conjugation.

2.2.1 Multiuser SIMO Channel Model

The multiuser SIMO underwater acoustic channel is derived from the communications channel between single elements. The model for the time-invariant underwater communications channel between a single, stationary transmitter and a single, stationary receiver can be described by

$$\begin{aligned} r(t) &= \int_{-\infty}^{\infty} h(\tau)s(t-\tau)d\tau + w(t) \\ &= h(t) * s(t) + w(t) \end{aligned} \tag{2.1}$$

where a transmission of $s(t)$ experiences $h(t)$, the overall channel response with delay parameter t, and additive, white-Gaussian noise, $w(t) \sim \mathcal{N}(0, N_0)$, at the receiver.

The time-invariant channel model between a single transmitter and a receiving array is derived from (2.1) for each element of the receiving array. The received signal on the i^{th} receiving element can be modeled as

$$r_i(t) = h_i(t) * s(t) + w_i(t), \tag{2.2}$$

where $h_i(t)$ represents the acoustic communication channel between the single user and the i^{th} element in the array and is assumed to be constant over the communications packet. The noise on the i^{th} element, $w_i(t)$ is assumed to be uncorrelated from the noise on all other elements.

The multiuser SIMO model can be obtained from the single user version in (2.2) with the addition of transmissions from independent users. The received

signal at the i^{th} element from simultaneous transmissions from M total users is given by

$$r_i(t) = \sum_{k=1}^{M} e^{j\phi_k(t)} h_i^k(t) * s_k(t - \Delta_k) + w_i(t), \tag{2.3}$$

in which, $h_i^k(t)$ represents the overall communications channel experienced by the transmitted signal from user k, $s_k(t)$, and the i^{th} receiver. A user-dependent phase rotation, $\phi_k(t)$, is introduced to describe differences in sampling and carrier frequency generation between each user and the receiver. Modeling the carrier frequency and sampling offsets in this manner implies a narrowband assumption on the transmitted signal, and may need to be modified for broadband signals. Because the users are assumed to communicate to the receiver independently (i.e. without cooperation), both the transmitted signal and the relative transmission delay from user k are assumed to be independent from all other users.

The underwater acoustic communication channel is known to be highly dispersive. An example of the impulse response between a single transmitter and a receiving array from FAF-06 is shown in Fig. 2.9a, indicating a delay spread of 30 ms or 120 symbol periods when transmitting 4 ksymbols per second. With multiple transmitters operating in a dispersive environment, the multiple access interference (MAI) scales not only with the total number of users, but also the number of nonzero components in the multipath delay profile, with a net effect of increasing the perceived MAI in the system. In combatting both the MAI and ISI of such channels, previous work based on DFE architectures has proved successful in jointly minimizing both interference components [1]. However, the two interference components are inherently different, and the focus of this paper is to distinguish the two interference components and remove them separately. First, a passive time-reversal combiner will mitigate partially the ISI and MAI for each user. Following the combiner, an interference cancellation technique will incrementally remove the remaining MAI for each user in the system. Finally, a single channel DFE will remove the residual ISI.

2.2.2 Passive Time-Reversal

One way of dealing with the increased ISI of the underwater acoustic channel is the combination of a simple channel estimation technique, e.g. a channel probe prepended to the data packet, and a passive time-reversal combiner that has been studied extensively in recent years [23].

A block diagram of passive time-reversal for a two user system is shown in Fig. 2.1. Passive time-reversal requires knowledge of the channel response between each user and the receiving array to create a filter bank that will focus the array on a particular user in space and time. The tap coefficients of each filter in a particular bank (e.g., $h_i^k(-t)$) are the time-reversed version of the channel response between the target user k and the corresponding receiver in the array. The outputs of the each filter bank are coherently combined to produce a single signal for each user, $y_k(t)$. Thus, the time-reversal approach provides the initial separation of the whole channel into parallel channels, one for each transmitting user. When applied to the multiuser SIMO model in (2.3), the overall communications model for the k^{th} user after time-reversal combining becomes

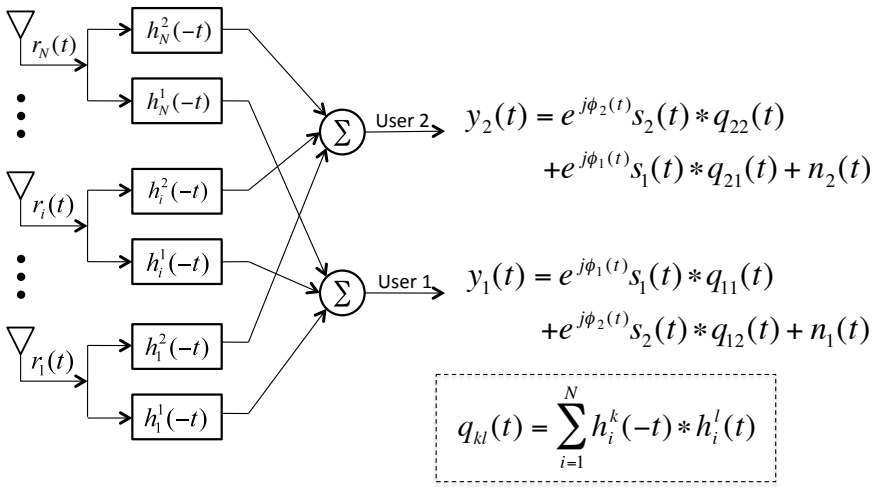

Figure 2.1: Block diagram for time-reversal combining in a two user system.

$$y_k(t) = \sum_{i=1}^{N} h_i^{k\dagger}(-t) * r_i(t) \tag{2.4}$$

$$= \sum_{l=1}^{M} e^{j\phi_l(t)} \left[\sum_{i=1}^{N} h_i^{k\dagger}(-t) * h_i^{l}(t) \right] * s_l(t - \Delta_l) + \sum_{i=1}^{N} h_i^{k\dagger}(-t) * w_i(t) \tag{2.5}$$

$$= e^{j\phi_k(t)} q_{kk}(t) * s_k(t - \Delta_k) + \sum_{l,l\neq k}^{M} e^{j\phi_l(t)} q_{kl}(t) * s_l(t - \Delta_l) + n_k(t), \tag{2.6}$$

where

$$n_k(t) = \sum_{i=1}^{N} h_i^{k\dagger}(-t) * w_i(t) \tag{2.7}$$

is a colored noise process, and

$$q_{kl}(t) = \sum_{i=1}^{N} h_i^{k\dagger}(-t) * h_i^{l}(t) \tag{2.8}$$

is known as the q-function between users k and l from the combination of N total receive elements [23]. When $l = k$, the q-function represents the sum of the autocorrelation functions of the communication channels between user k and the receiving array. However, when $l \neq k$, the q-function describes the interference caused by user l when focusing the array on user k. In an ideal, interference-free scenario, $q_{kk}(t) = \delta(t)\ \forall\ k$, and $q_{kl}(t) = 0\ \forall\ l \neq k$. An example of the q-functions in a 2-user system is shown in Fig. 2.9b. The peak in the top panel corresponds to the q-function resulting from alignment of the time-reversal combiner to the desired user. The bottom panel illustrates an example of the interfering q-function between differing users.

Assuming optimal sampling of the output of the time-reversal combiner, each user's transmission experiences an array gain equal to the squared magnitudes of all non-zero channel tap values. In this way, time-reversal combining can be viewed as a generalization of maximal-ratio combining (MRC) for scalar channels, in which a user's transmission experiences an array gain equal to the sum of the squared magnitudes of the single channel tap value to each array element. However, in the presence of interference, passive time-reversal focuses the receiver array to each particular user, creating parallel – but not interference-free – channels

at its output [23]. In addition to an array gain and limited interference suppression, passive time-reversal offers another beneficial quality for communications. Specifically, it can shorten the effective channel impulse response, $q_{kk}(t)$. When used as a receiver preprocessor, time-reversal combining can lower the computational complexity on all following processing, but more importantly, it preserves the spatial degrees of freedom necessary for multiple access communications [30].

2.2.3 Interference Model

From (2.6), we can describe the output of time-reversal combining in Fig. 2.1 for the k^{th} user as the sum of three quantities,

$$y_k(t) = e^{j\phi_k(t)} q_{kk}(t) * s_k(t - \Delta_k) + i_k(t) + n_k(t). \tag{2.9}$$

The first component represents the desirable output of the time-reversal preprocessor focused to user k. The third component, $n_k(t)$, represents a colored Gaussian noise process. The second component describes the interference caused by all other users $l \neq k$, and is expressed as

$$i_k(t) = \sum_{l,l\neq k}^{M} i_{kl}(t) = \sum_{l,l\neq k}^{M} e^{j\phi_l(t)} q_{kl}(t) * s_l(t - \Delta_l). \tag{2.10}$$

The previous expressions can be used to derive an important performance metric for multiuser systems, the signal-to-interference-plus-noise ratio (SINR). The SINR for a specific user k at the output of the time-reversal combiner is given by

$$\mathrm{SINR}_k = \left(\mathrm{SIR}_k^{-1} + \mathrm{SNR}_k^{-1}\right)^{-1} \tag{2.11}$$

where

$$\mathrm{SIR}_k = \frac{P_k \int |q_{kk}(t)|^2 \, dt}{\sum_{l,l\neq k}^{M} P_l \int |q_{kl}(t)|^2 \, dt} \tag{2.12}$$

is the signal-to-interference ratio,

$$\mathrm{SNR}_k = \frac{P_k}{N_0} \cdot \frac{\int |q_{kk}(t)|^2 \, dt}{\sum_{i=1}^{N} \int \left|h_i^k(t)\right|^2 \, dt} \tag{2.13}$$

is the signal-to-noise ratio, and P_k is the average transmit power for user k. Detailed derivations of these expressions are given in Appendix 2A.

In a single-user scenario ($M = 1$), SIR $= \infty$, and SINR = SNR. Although passive time-reversal maximizes SNR (and thus SINR) in a single user setting, it *does not* jointly maximize both the SNR and SIR and thus *does not* maximize SINR in a multiuser setting. Additionally, inspection of the previous expressions show that in the interference dominant regime (i.e., $\text{SIR}_k \ll \text{SNR}_k$), the overall system performance does not improve by allowing users to trivially increase their transmission power, P_k.

2.3 Receiver Architecture: Passive Time-Reversal and Successive Interference Cancellation

An intelligent receiver can estimate $i_k(t)$, described in Sec. 2.2.3, to remove multiuser interference before making symbol decisions. Ideally, the interference component of the SINR can be removed, and the SNR gain provided by time-reversal can be preserved. One such capable design is Successive Interference Cancellation (SIC), in which the receiver subtracts interference caused by all previously decoded users prior to decoding the target user. By iterating the SIC process, SIR_k can potentially be driven toward infinity for all k, allowing SINR_k to approach SNR_k for all k, and symbol estimates to be improved for all users. In the context of wireless applications, the linear MMSE (minimum mean-squared error) receiver with SIC decoding and proper power allocation has proven to achieve the capacity of the i.i.d. scalar Rayleigh fading channel [31, pp. 355-364]. This startling fact motivates its application for multiuser interference cancellation in the underwater setting.

A block diagram for the SIC process for underwater communications is shown in Fig. 2.2. Initially, passive time-reversal is applied to the multichannel received signals to transform the dispersive multiuser SIMO channel into a

compressed multiuser SISO channel (see Fig. 2.1). Then, SIC is applied to the ensemble of SISO channels, $y_k(t), k = 1, \ldots, M$. However, the SIC process cannot be applied blindly. The interference cancellation architecture must be modified to incorporate the effects of time-reversal processing. Namely, because multichannel combining occurs at the beginning of the receiver, multiuser interference estimates must also be modeled after time-reversal processing. This is done by combining co-user symbol information with interfering q-function estimates.

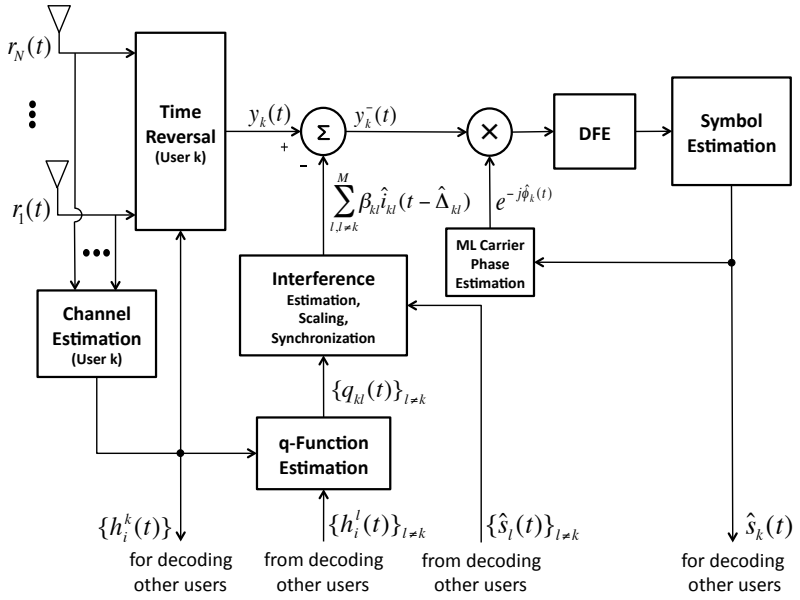

Figure 2.2: Block diagram of Successive Interference Cancellation for decoding the k^{th} user with channel and symbol information learned by first decoding competing users.

During the initialization phase of SIC, a decoding order is chosen. Then, each user's signal after time-reversal combining, $y_k(t)$, is enhanced in succession through interference estimation, synchronization, scaling and cancellation with respect to previously decoded users and their respective cross q-functions. Once the interference is removed from the desired user's signal, residual ISI is removed with the aid of a DFE before symbol decisions are made. This process can be repeated, with symbol estimates updated at each iteration, until a stationary point

is reached or a sufficient number of iterations have passed.

The following descriptions elaborate on each component of SIC.

1) Decoding Order Selection

The users should be ordered by decreasing SINR at each iteration. This minimizes the effect of error propagation through the SIC process. Therefore, at each iteration, the users with the largest SINRs should be decoded first, allowing users with smaller SINRs to take advantage of more accurate interference estimates. Note that during the first iteration the interference cannot be estimated for the first user in the sequence. This user's message must be decoded using previously developed methods in [23], i.e. time-reversal combining followed by decision-feedback equalization.

2) Interference Estimation

For the other users in the first iteration and for all users in the following iterations, the quantities described in (2.10) can be combined to form an interference estimate for each interfering user. When decoding a user k in the presence of a previously decoded interferer, user $l \neq k$, an interference estimate is formed as

$$\hat{i}_{kl}(t) = e^{j\hat{\phi}_l(t)} q_{kl}(t) * \hat{s}_l(t), \tag{2.14}$$

where $\hat{\phi}_l(t)$ is the estimate of the phase rotation for the l^{th} user, which will be described shortly. The q-function between users k and l is formed from the channel estimates of the respective users, and $\hat{s}_l(t)$ is provided by the output of the symbol estimation block for that user.

3) User Synchronization

In general, each user's signal will arrive at the receiving array at a different time, represented in the original model by $\{\Delta_k\}$. In practice, the interference estimates must be synchronized to their respective signals, and only relative delays need to be considered. This is achieved by matched-filtering each of

the interference estimates in (2.14) to the target user's signal such that

$$\alpha_{kl}(t) = \hat{i}_{kl}(-t) * y_k(t) \tag{2.15}$$

$$\hat{\Delta}_{kl} = \arg\max_{\tau} \ |\alpha_{kl}(\tau)|^2 , \tag{2.16}$$

where $\hat{\Delta}_{kl}$ represents the transmission delay of user l with respect to user k.

4) Interference Scaling

In an ideal scenario, one in which the receiver has error-free knowledge of $s_l(t)$ and a perfect estimate of $q_{kl}(t)$, the interference estimate would be exact and could be synchronized to and directly subtracted from the target user's $y_k(t)$. However, with only estimates of these quantities available, a more careful examination is required. A scaling factor for the interference, given by

$$\beta_{kl} = \frac{\alpha_{kl}(\hat{\Delta}_{kl})}{1 + \mathrm{SNR}_k^{-1} \cdot \frac{P_k \int |q_{kk}(t)|^2 dt}{P_l \int |q_{kl}(t)|^2 dt}} \tag{2.17}$$

can provide the necessary balance between interference cancellation and noise enhancement. A derivation for β_{kl} is given in Appendix 2B. With poor estimates of $s_l(t)$ and the channel response (and thus, the q-functions), the maximal output of the synchronizer $\alpha_{kl}(\hat{\Delta}_{kl})$ will be low and β_{kl} will take a minimal value. Additionally, in the low-SNR limit with respect to the interference power, β_{kl} will also take a minimal value. Only in the high-SNR limit with respect to the interference power will the denominator of β_{kl} converge to 1, leading to the full-scale removal of the estimated interference out of the time-reversal combiner.

5) Cancellation

Following estimation, scaling, and synchronization of all interference, the improved, target signal is obtained by simple subtraction,

$$y_k^-(t) = y_k(t) - \sum_{l,l\neq k}^{M} \beta_{kl} \hat{i}_{kl}(t - \hat{\Delta}_{kl}). \tag{2.18}$$

6) Equalization and Decoding

Upon successful cancellation of interference, $y_k^-(t)$ corresponds to the conventional, time-reversal combined reception of a single user's signal in an interference-free environment. Although time-reversal combining reduces the amount of effective delay spread, residual ISI is still present. Thus, a DFE is employed to mitigate the remaining ISI. The interference-free and ISI-free signal at the output of the DFE is then decoded to produce updated symbol estimates for the k^{th} user, as shown in Fig. 2.2. At this point, an error-correcting code could be introduced prior to the feedback of symbol information to further improve the quality of the interference estimates. After applying an error-correcting decoder, the information bits would be re-encoded to generate an estimate of the transmitted symbols to be fed back for cancellation.

Following time-reversal combining and SIC, a decision-feedback, maximum-likelihood (ML) carrier phase estimator [9] is used to correct the phase rotation for the k^{th} user, denoted $\hat{\phi}_k(t)$. During the first iteration, when a previous version of $\hat{s}_k(t)$ is unavailable to the receiver, training symbols are used to estimate $\phi_k(t)$ for $t < T_{\text{P}}$, where T_{P} is the duration of the preamble, and a linear extrapolation is performed for the data-bearing portion of the packet. For the following iterations, the most recent version of $\hat{s}_k(t)$ is used as a reference for the phase estimation, leading to improved estimates of $\phi_k(t)$ with successive iterations.

It is important to note that the availability of reliable channel estimates between each user and the receiving array has been assumed. In previous work on time-reversal communications, a channel probe was prepended to the data packet to initialize the time-reversal mirror [23]. However, with a set of asynchronous users, independent receptions of channel probes cannot be guaranteed. In fact, as the number of users grows large, the probability that a channel probe is received without MAI becomes low and some protection must be incorporated for these highly-probable events. Recent work on the subject has demonstrated that channel estimation from multiple-source transmissions of channel probe signals is possible with careful design of the probing signals [32], although to the authors'

knowledge, this work has also been limited to time-invariant channels. For the data processed in the following section, independent (MAI-free) receptions of channel probes from all users were provided by experiment design, and the necessary relaxation of this implicit synchronization of otherwise independent users is the subject of ongoing research. More generally, the applicability of matched-filter receivers in time-varying channels (especially the multiple-access channel) is the subject of ongoing research.

2.4 Experimental Results

The iterative SIC decoding procedure was analyzed using experimental data collected in the Focused Acoustic Fields experiments during 2005 and 2006. The following sections detail the experiment setup and parameters and provide results of iterative SIC decoding on receptions of simultaneous, multiuser transmissions through shallow water environments. In the interest of reporting raw bit-error rates, error-correcting codes were not introduced prior to the feedback of symbol information in the SIC process. Instead, quantized symbol estimates out of the equalizer were directly fed back for interference cancellation. It should be noted that both of the data examples presented in the next sections exhibited little-to-no time variation of the channel experienced by each user to the array upholding the assumptions made in the derivation of the receiver architecture in Section 2.2.

2.4.1 Focused Acoustic Fields 2005

The FAF-05 Experiment was conducted in cooperation with the NATO Undersea Research Center in July 2005, north of Elba Island off the west coast of Italy. Communications packets were transmitted simultaneously from three users (3-element subset of a source array), through a 120-m deep water column to a 20-element vertical receiving array (VRA), as shown in Fig. 2.3. For the data discussed in the following analysis, the VRA was located 20 km from the users. The VRA interelement spacing was 2-m with Element 1 at a 110-m depth. Further details on the FAF-05 experiment are available in [23].

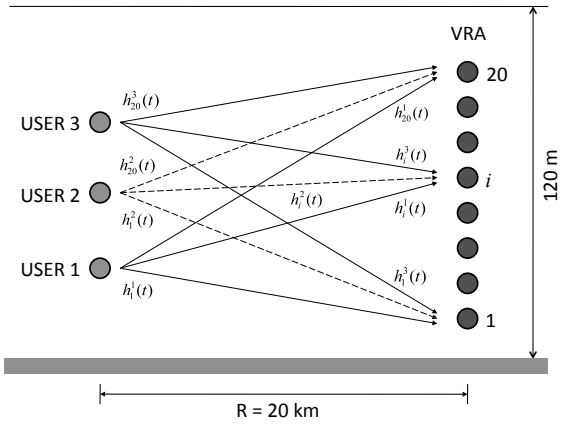

Figure 2.3: FAF-05 experiment setup. User 1 (113-m deep), User 2 (101-m deep), and User 3 (88-m deep) transmit to a 20-element receiving array with inter-element spacing of 2 m and Element 1 at a depth of 110 m.

After independent transmissions of a 300-ms LFM chirp (over the 2.5-4.5 kHz band) as a channel probe, each user transmitted an 8-second packet of 16-QAM symbols using LFM pulses over the 3-4 kHz frequency band. With each user transmitting at a rate of 500 symbols per second with a 10% training overhead, the overall, system-wide transmission rate was 5.4 kbps with a spectral efficiency of 5.4 b/s/Hz. An estimate of the channel impulse response between each of the three users and the array, required to initialize both the time-reversal combiner and SIC process, were obtained by matched-filtering to the independent channel probes. An example of the result of such processing for a single user is provided in Fig. 2.4. Because the channel was assumed to remain unchanged throughout the data packet, these estimates were not re-estimated in a data-directed fashion. The feedforward and feedback filters of the single-channel DFE were initialized with 16 fractionally-spaced and 4 symbol-spaced taps, respectively. The equalizer taps were updated using the recursive least-squares (RLS) algorithm with a forgetting-factor of 0.99. Decoding after time-reversal combining alone, as in [23], resulted in an aggregate, system-wide bit-error rate (BER) of 1.53×10^{-2}, as shown in Fig. 2.5 (top). After 3 iterations of interference cancellation, the error rate was improved to 8.80×10^{-4}, as shown in Fig. 2.5 (bottom). The system-wide aggregate SNR at the output of the equalizers, calculated as the inverse of the mean-squared error for

all transmitted symbols, was increased from 13.71 dB to 18.01 dB. A user-by-user summary of the performance of the algorithm is provided in Table 2.1.

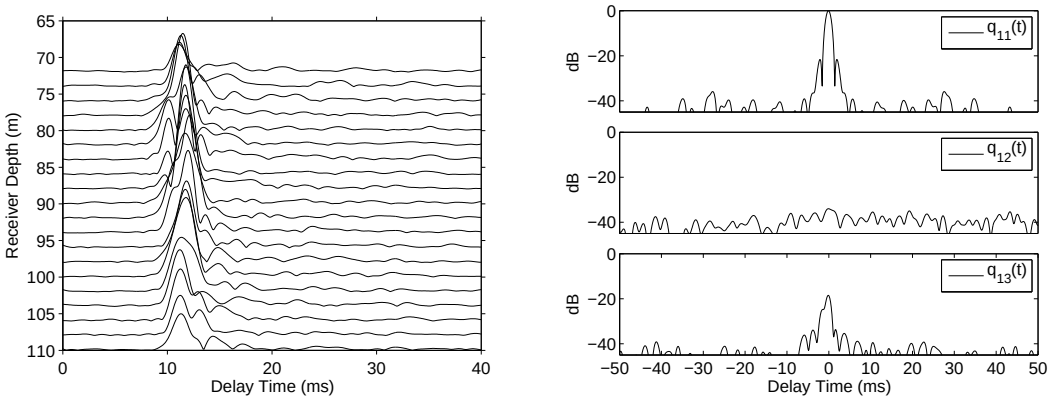

(a) (b)

Figure 2.4: (a) A single user's complex-baseband equivalent channel impulse response measured during FAF-05 indicating a delay spread of about 10 ms, and (b) corresponding q-functions resulting from a 3-user system in this environment; (top) $q_{11}(t)$ - output of time-reversal mirror aligned to desired user; (middle) $q_{12}(t)$ - interference from a competing user; (bottom) $q_{13}(t)$ - interference from another competing user.

Figure 2.6 illustrates the output SNR after each iteration and all combinations of decoding order. For this particular example, the order of decoding did not impact the final results. Every choice leads to similar decoding of all users in a small number of iterations. Apparently, time-reversal combining provides enough interference suppression to decode each user, avoiding catastrophic error propagation. However, this is not the case in general, and a careful ordering of users will be required in most circumstances as described in Section 2.3, especially in circumstances where the imbalance of received powers is more dramatic than that of this example.

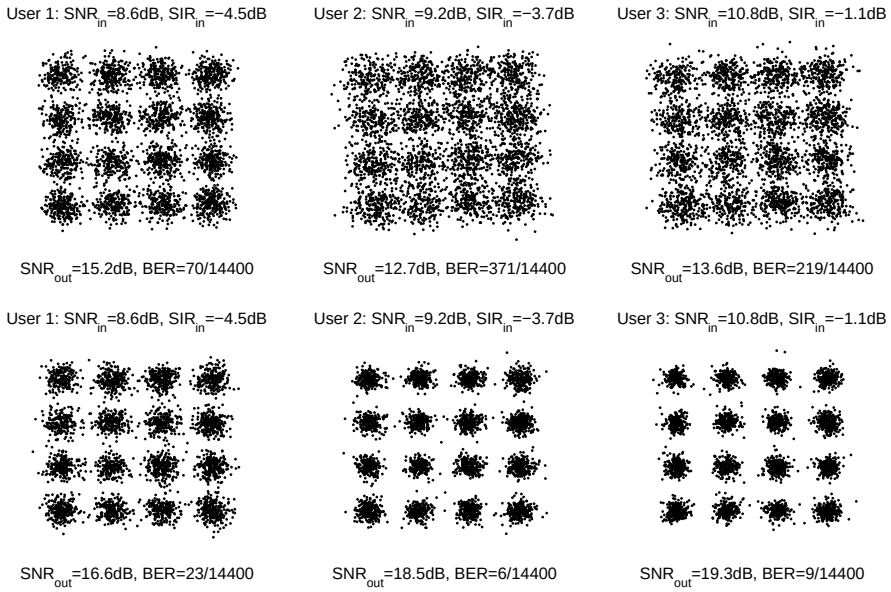

Figure 2.5: Decoding improvement for the 3-user system from FAF-05 shown in Fig. 2.3: (top) after time-reversal combining and decision-feedback equalization, and (bottom) after time-reversal combining, 3 iterations of SIC, and decision-feedback equalization.

2.4.2 Focused Acoustic Fields 2006

The FAF-06 Experiment, conducted south of Elba Island, explored a higher frequency band (9-21 kHz) and thus higher-rate communications in a downslope environment, as shown in Fig. 2.7. The experiment allowed for two users in 46-m deep water to transmit simultaneous communications packets to a 16-element vertical receiving array placed at a range of 2.2 km and in 92-m water depth. The VRA interelement spacing was 3.75-m with Element 1 at a 25-m depth. As shown in Fig. 2.8, the higher bandwidth and shorter range led to a more multipath-rich and dispersive environment than that encountered in FAF-05, with a channel exhibiting a delay spread of approximately 30 ms. In comparison, most of the multipath arrivals during FAF-05 were confined to a few milliseconds before and after the dominant arrival. Further details on the FAF-06 experiment are available in [33].

Table 2.1: Element-Level Input SNR/SIR and Output SNR for FAF-05 and FAF-06

User	FAF-05			FAF-06		
	SNR_{in}	SIR_{in}	SNR_{out}	SNR_{in}	SIR_{in}	SNR_{out}
1	8.6 dB	-4.5 dB	16.6 dB	18.7 dB	1.9 dB	19.4 dB
2	9.2 dB	-3.7 dB	18.5 dB	16.9 dB	-1.9 dB	17.8 dB
3	10.8 dB	-1.1 dB	19.3 dB	–	–	–

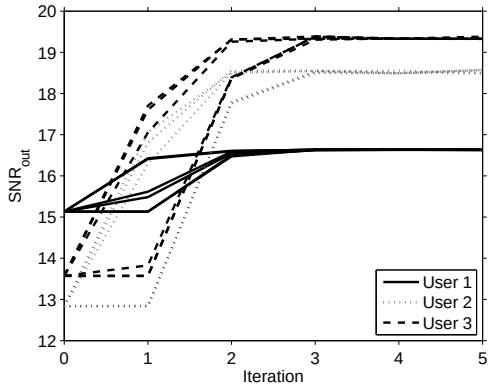

Figure 2.6: Output SNR after each iteration for every possible decoding order for the FAF-05 data example.

Similar to the FAF-05 experiment, both users transmitted a single 60-ms LFM channel probe followed by a 2.4 sec communications sequence of 8-QAM symbols at a rate of 4000 symbols per second shaped with LFM pulses over the 9-21 kHz frequency band. The total, system-wide throughput for this experiment, again assuming a 10% overhead for training purposes, was 21.6 kbps with a spectral efficiency of 1.8 b/s/Hz. Similar to the processing of the FAF-05 data, the initial channel impulse response estimates between each user and the array were obtained by matched-filtering to the independent channel probes. An example of the channel impulse response between a single user and the array as well as the associated q-functions are presented in Fig. 2.9. The feedforward and feedback filters of the DFE were initialized with 24 fractionally-spaced and 16 symbol-spaced taps, respectively, and were updated with the RLS algorithm with a forgetting-factor

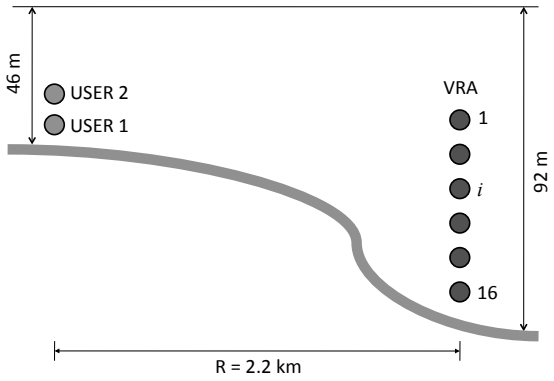

Figure 2.7: FAF-06 experiment setup. User 1 (43.8-m deep) and User 2 (39.6-m deep) transmit to a 16-element receiving array at 2.2-km range with an inter-element spacing of 3.75 m and Element 1 at a depth of 25 m.

of 0.999. The received packets were decoded, after time-reversal processing and decision-feedback equalization only, and again after three iterations of interference cancellation. The results of the processing, as seen in Fig. 2.10, show an aggregate bit-error rate improvement from 1.77×10^{-3} to error-free decoding, and an aggregate SNR increase from 13.79 dB to 18.55 dB. A user-by-user summary is provided in Table 2.1.

2.4.3 Performance in Low SNR Environments

During each of the experiments, an ensemble of twenty noise recordings were collected immediately prior to the data segments of interest. One at a time, these noise recordings were scaled and added to the data to achieve a desired decrease in input SNR (relative to the original input SNR, see Table 2.1), and the sum was used to first estimate the channel between each user and the array and subsequently decoded using the SIC procedure. The result of this processing produced twenty output SNR's at each reduced input SNR value. An aggregate performance was reported as the average performance (in mean-squared error space) of the twenty decodings at each input SNR. Fig. 2.11 shows the performance decline for each of the users as the input SNR was decreased for the data recordings from both experiments. For comparison purposes, the same analysis was performed using the

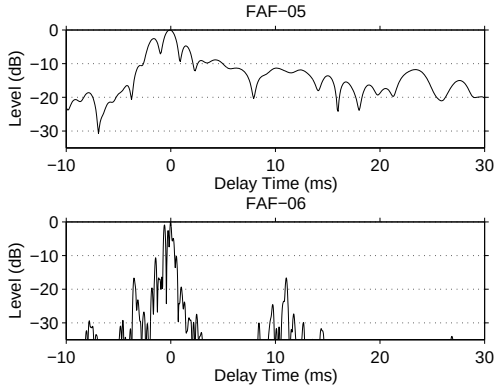

Figure 2.8: Comparison between the channel impulse response experienced between a single user and a single receive element during the FAF-05 and FAF-06 experiments.

decentralized reduced-complexity multichannel DFE first proposed in [1], and the results are shown by the gray curves in Fig. 2.11. For the FAF-05 data, 4 combiner vectors were used (P in [1]), with feedforward and feedback filters consisting of 32 and 4 taps, respectively. Both the combiner and equalizer taps were updated using the standard RLS algorithm with a forgetting-factor of 0.999. For the FAF-06 data, a P of 16 was used, with feedforward and feedback filters consisting of 2048 and 0 taps, respectively. The dramatic increase in the number of taps was a necessary consequence of the more dispersive nature of the FAF-06 channel response coupled with a higher symbol rate. The combiner for the FAF-06 analysis was updated using the standard RLS algorithm with a forgetting-factor of 0.999 while the linear equalizer was updated using the normalized LMS algorithm with step size 0.5.

Because the iterative SIC approach was able to use symbol information from the stronger users to improve the decoding performance for the weaker users (see Table 2.1), the performance decline as the SNR was decreased was nearly uniform. The presence of a stronger user was not detrimental to the decoding performance for the weaker users, since the interference estimate from the stronger user led to more accurate interference estimates and thus more effective interference cancellation. In other words, weaker users were not sacrificed in the low-SNR limit, and the SIC approach appears to be capable of dealing with the near-far problem inherent

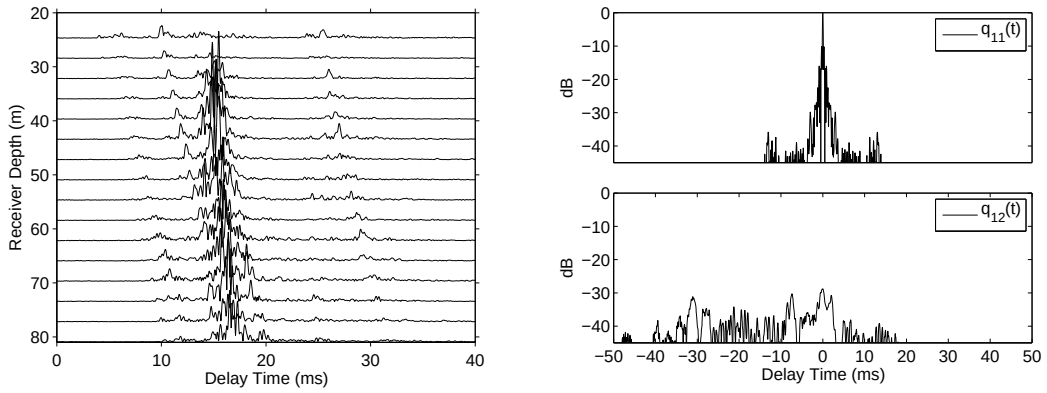

(a) (b)

Figure 2.9: (a) A single user's complex-baseband equivalent channel impulse response measured during FAF-06 indicating a delay spread of about 30 ms, and (b) corresponding q-functions resulting from a 2-user system in this environment; (top) $q_{11}(t)$ - output of time-reversal mirror aligned to desired user; (bottom) $q_{12}(t)$ - interference from a competing user.

in the underwater acoustic channel which exhibits heavily range-dependent fading. Moreover, a robustness to the near-far problem is a feature already observed in this method's cellular counterpart [27], and makes this approach a natural candidate for combatting the problem for underwater acoustic multiuser detection.

2.5 Summary and Conclusions

In order to support simultaneous acoustic transmissions from multiple users in an underwater setting, a separation scheme was employed for successful multiple-access communications. For the uplink underwater acoustic channel, the burden of multiuser separation was passed to the receiver, where the problem was first simplified by introducing a passive time-reversal combiner. Following time-reversal, Successive Interference Cancellation removed the interference caused by competing users to create an ensemble of parallel, interference-free channels. SIC was shown to be the multiuser interference equivalent of the decision-feedback equalizer for

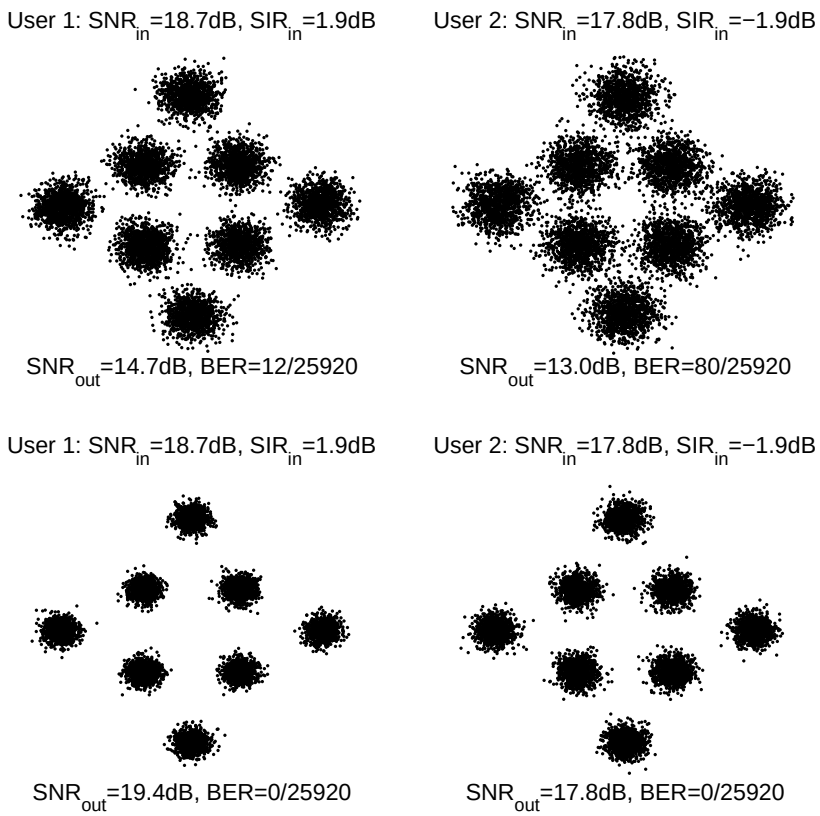

Figure 2.10: Decoding improvement for the 2-user system from FAF-06 shown in Fig. 2.7: (top) without SIC, and (bottom) after 4 iterations of SIC.

intersymbol interference channels. The DFE uses interfering symbol estimates and knowledge of the channel to remove the distortion caused by neighboring symbols, whereas SIC performed the same process using symbol estimates from interfering users and q-function estimates from time-reversal combining. With a small number of iterations of the SIC procedure, symbol estimates were improved for each user, leading to more accurate estimates of the interference experienced by competing users. The overall effect was a boost in the output SNR for all users.

Analysis of experimental data demonstrated the effectiveness of the interference cancellation scheme. The simple SIC design presented in this paper was shown to improve the decoding performance of communications data collected during the FAF-05 and FAF-06 experiments. For a 3-user communications packet

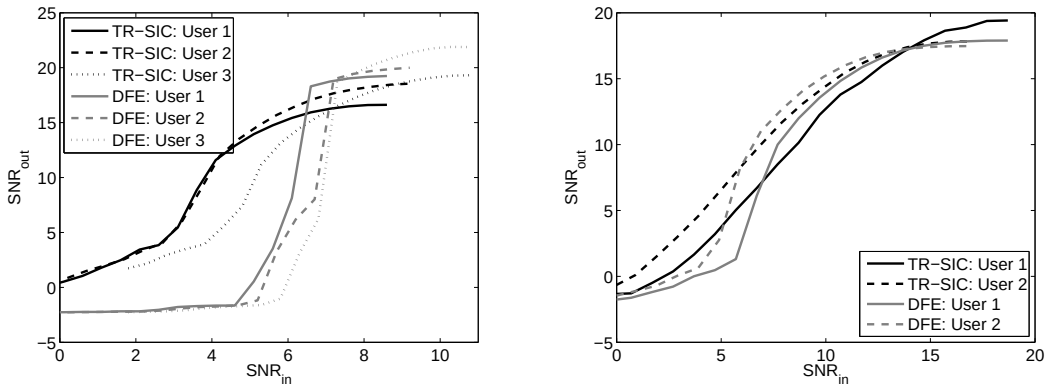

(a) (b)

Figure 2.11: Performance of the iterative SIC multiuser detector as the element-wise input SNR is reduced relative to the original data recordings for the (a) FAF-05 and (b) FAF-06 data examples. The black curves correspond to the performance of the proposed multiuser detector while the gray curves depict the performance of the decentralized multiuser detector in [1]. The rightmost data point in each curve corresponds to results of processing the original recording.

collected during FAF-05, time-reversal combining followed by equalization led to a BER of 1.53×10^{-2} and an output SNR of 13.7 dB, while 3 iterations of SIC improved these results to a BER of 8.80×10^{-4} and an output SNR of 18.0 dB. For a 2-user, broadband communications packet collected during FAF-06, time-reversal combining followed by equalization led to a BER of 4.76×10^{-2} and an output SNR of 13.5 dB. SIC was able to enhance the decoding performance to an error-free level with an output SNR of 18.55 dB, after 4 iterations.

Acknowledgements

This work was supported by the Office of Naval Research under grant N00014-07-1-0739.

Chapter 2, in full, is a reprint of the material as it appears in "Successive Interference Cancellation for Underwater Acoustic Communications, S. E. Cho,

H. C. Song, and W. S. Hodgkiss, *IEEE Journal of Oceanic Engineering*, Vol. 36, No. 4, August 2011, pp. 490–501. The dissertation author was the primary investigator and author of this paper.

2A Derivation of SINR$_k$

Constructing the ratio of the expected signal power to the expected interference and noise power from (2.9) gives the SINR for the k^{th} user at the output of the time-reversal combiner as

$$\text{SINR}_k = \frac{E\left[\int |q_{kk}(t) * s_k(t-\Delta_k)|^2\, dt\right]}{E\left[\int |i_k(t)+n_k(t)|^2\, dt\right]} \tag{2.19}$$

$$= \frac{E\left[\int |q_{kk}(t) * s_k(t-\Delta_k)|^2\, dt\right]}{E\left[\int \left|\sum_{l,l\neq k}^{M} q_{kl}(t) * s_l(t-\Delta_l)\right|^2 dt\right] + E\left[\int |n_k(t)|^2\, dt\right]}, \tag{2.20}$$

under independence assumptions between signal and noise components.

Assuming $s_k(t)$ is wide-sense stationary (WSS) with autocorrelation function

$$R_k(\tau) = P_k \cdot \delta(\tau), \tag{2.21}$$

where P_k is the average transmit power for user k, the numerator of (2.20) can be expressed as

$$E\left[\int |q_{kk}(t) * s_k(t-\Delta_k)|^2\, dt\right] = P_k \cdot T \int |q_{kk}(t)|^2\, dt, \tag{2.22}$$

where T is the total transmission time.

For $l \neq m$, the transmitted signals are assumed to be independent, thus

$$E\left[s_l^{\dagger}(t-\Delta_l) s_m(t-\Delta_m)\right] = E\left[s_l^{\dagger}(t-\Delta_l)\right] E\left[s_m(t-\Delta_m)\right] = 0, \tag{2.23}$$

and the first term in the denominator of (2.20) can be reduced to

$$E\left[\int \left|\sum_{l,l\neq k}^{M} q_{kl}(t) * s_l(t-\Delta_l)\right|^2 dt\right] = \sum_{l,l\neq k}^{M} E\left[\int |q_{kl}(t) * s_l(t-\Delta_l)|^2 dt\right] \tag{2.24}$$

$$= T \sum_{l,l\neq k}^{M} P_l \int |q_{kl}(t)|^2\, dt. \tag{2.25}$$

Similarly, because $n_k(t)$ can be described as a combination of filtered WSS processes,

$$n_k(t) = \sum_{i=1}^{N} h_i^k(t) * w_i(t), \tag{2.26}$$

where $w_i(t) \sim \mathcal{N}(0, N_0)$ with $w_i(t) \perp w_j(t)$ for $i \neq j$, the noise component of (2.20) can be reduced to

$$E\left[\int |n_k(t)|^2 \, dt\right] = \int E\left[\left|\sum_{i=1}^{N} h_i^k(t) * w_i(t)\right|^2\right] dt \tag{2.27}$$

$$= N_0 \cdot T \sum_{i=1}^{N} \int \left|h_i^k(t)\right|^2 dt. \tag{2.28}$$

Combining the previous expressions, the expression for SINR becomes

$$\mathrm{SINR}_k = \frac{P_k \cdot T \int |q_{kk}(t)|^2 \, dt}{T \sum_{l,l\neq k} P_l \int |q_{kl}(t)|^2 \, dt + N_0 \cdot T \sum_{i=1}^{N} \int \left|h_i^k(t)\right|^2 dt} \tag{2.29}$$

Denoting

$$\mathrm{SIR}_k = \frac{P_k \int |q_{kk}(t)|^2 \, dt}{\sum_{l,l\neq k}^{M} P_l \int |q_{kl}(t)|^2 \, dt} \tag{2.30}$$

as the signal-to-interference ratio, and

$$\mathrm{SNR}_k = \frac{P_k}{N_0} \cdot \frac{\int |q_{kk}(t)|^2 \, dt}{\sum_{i=1}^{N} \left|h_i^k(t)\right|^2 dt}, \tag{2.31}$$

as the signal-to-noise ratio, the signal-to-interference-plus-noise ratio for user k becomes

$$\mathrm{SINR}_k = \frac{1}{\mathrm{SIR}_k^{-1} + \mathrm{SNR}_k^{-1}}. \tag{2.32}$$

2B Derivation of β_{kl}

Let y be the received value of the scalar transmission of a random variable x, through a channel with zero-mean interference i, before experiencing AWGN with distribution $\mathcal{N}(0, N_0)$. That is,

$$y = x + \alpha i + n, \tag{2.33}$$

where α is a measure of the severity of the interference. At the receiver, an estimate of the interference is available in the form of

$$\hat{i} = i + w, \tag{2.34}$$

where w is also distributed $\mathcal{N}(0, N_0)$, i.e. $\hat{i}$ is a noisy measurement of the interference taken at the receiver. The receiver cancels the interference by scaling and subtracting it from y to form

$$y^- = y - \beta_{\text{MMSE}}\hat{i}, \tag{2.35}$$

where β_{MMSE} is chosen to minimize the mean-squared error. That is,

$$\beta_{\text{MMSE}} = \arg\min_{\beta} E\left[\left|y - \beta\hat{i}\right|^2\right], \tag{2.36}$$

which is uniquely found by solving the following equation

$$\frac{\partial}{\partial\beta} E\left[\left|y - \beta\hat{i}\right|^2\right] = 0. \tag{2.37}$$

The solution for the scalar scenario is

$$\beta_{\text{MMSE}} = \frac{\alpha}{1 + \frac{N_0}{\text{var}(i)}}. \tag{2.38}$$

The solution for the continuous case in which the receiver desires to cancel interference from user l for the purposes of decoding user k similarly can be derived as

$$\beta_{kl} = \frac{\alpha_{kl}(\hat{\Delta}_{kl})}{1 + \frac{\int E\left[|n_k(t)|^2\right]dt}{\int E\left[|q_{kl}(t) * s_l(t)|^2\right]dt}} \tag{2.39}$$

$$= \frac{\alpha_{kl}(\hat{\Delta}_{kl})}{1 + \frac{N_0 \sum_{i=1}^{N} \int \left|h_i^k(t)\right|^2 dt}{P_l \int |q_{kl}(t)|^2 dt}} \tag{2.40}$$

$$= \frac{\alpha_{kl}(\hat{\Delta}_{kl})}{1 + \text{SNR}_k^{-1} \cdot \frac{P_k \int |q_{kk}(t)|^2 dt}{P_l \int |q_{kl}(t)|^2 dt}}, \tag{2.41}$$

where α_{kl} is defined in (2.15).

Chapter 3

Multiuser Interference Cancellation in Time-Varying Channels

In this letter, an adaptive time-reversal (ATR) multichannel combiner is embedded within an iterative successive interference cancellation (SIC) receiver. With the addition of matching pursuit (MP), a sparse channel estimation technique, the combined receiver is shown to provide both temporal interference cancellation as well as spatial interference suppression in decoding simultaneous transmissions from separate users in a time-varying underwater acoustic environment. Experimental data collected during the KAM11 experiment illustrates that for a 2-user multiple-access system, multiuser separation can be achieved.

3.1 Introduction

Following the introduction of adaptive decision-feedback equalization (DFE) for single-user communications through shallow water channels [17], time-reversal (TR) approaches have become a popular alternative for phase-coherent decoding [13, 34]. In rich multipath fading environments (e.g. the shallow water acoustic channel), TR approaches are particularly attractive for both the array gain from multichannel combining as well as the computational savings from a signifi-

cant intersymbol interference reduction at the output of the combiner. However, while adaptive DFE receivers are inherently capable of tracking a time-varying channel, TR receivers require a priori knowledge of the channel and must be supplemented with reliable channel estimation and tracking techniques. Previously, in cases where the channel could be modeled as time-invariant within a packet, channel estimates could be provided by a channel probe or training symbols prepended to a packet. When this assumption no longer held, i.e. time-varying channels, recent results showed that TR could also be applied with decision-directed channel updates and block-based processing [34, 21].

When considering multiple users, each with a single transmitter, communicating simultaneously to a single receiving array without the explicit use of time, frequency, or code division, extending either class of receivers became nontrivial. While an adaptive multiuser DFE was derived to address the problem, its implementation was limited by the exponential growth in computational complexity in the number of users [1]. On the other hand, within the TR domain, adaptive time-reversal (ATR) was developed as an approach for nulling multiple-access interference (MAI) from competing users while maintaining its beneficial qualities, e.g. computational efficiency [2]. In contrast to other TR approaches, ATR optimized the multichannel comber to minimize MAI while leaving the desired user's signal undisturbed at its output. Unfortunately, ATR shared the same characteristic as other TR techniques in that it also required knowledge of the channel prior to decoding. Because of this fact, ATR could not be extended directly to time-varying channels, because a means for channel estimation and tracking in the presence of strong MAI was not available.

In this letter, we will address this problem and develop the means for applying ATR in time-varying environments. The proposed receiver embeds ATR within an iterative, successive interference cancellation (SIC) framework. Using previously decoded symbols, SIC potentially can suppress MAI from competing users at the multichannel level, creating a limited MAI setting in which matching pursuit (MP), a sparse channel estimator [35], can perform channel updates. SIC has been heavily studied as a multiuser separation technique for wireless communi-

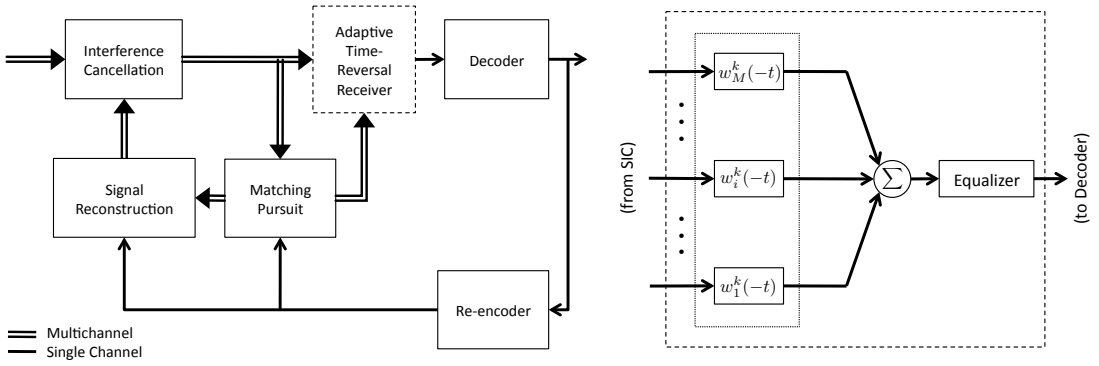

(a) (b)

Figure 3.1: (a) A receiver block diagram with ATR and MP embedded in the SIC framework. (b) The ATR receiver for decoding user k. The filter weights are designed to minimize crosstalk from competing users without distorting the signal from user k.

cations [27] and recently was considered for use in the (time-invariant) underwater acoustic channel [36]. Because SIC is a greedy approach, the increase in complexity was shown to be linear in the number of users. Even so, encouraging results showed SIC's capability and robustness when compared to other techniques, albeit in time-invariant environments.

The proposed receiver will be investigated with two-user data collected over the 20–30 kHz band during a recent experiment conducted in shallow water. With sufficient decoding iterations, the combination of SIC and MP will be capable of tracking a time-varying channel in the presence of strong MAI, providing ATR with the means to achieve multiuser separation.

3.2 Combined receiver: ATR and SIC

To extend the previous methods to time-varying channels, the standard block-wise processing approach will be considered, and the channel will be assumed time-invariant within each block. Each block will be decoded using the proposed architecture depicted in Fig. 3.1. MAI from transmissions during the

current and previous blocks will be partially mitigated by SIC, followed by sparse channel estimation with MP. Recently, it has been shown that for an L-tap channel with m nonzero components, matching pursuit techniques are capable of reliably estimating a sparse channel with $O(m \log L)$ measurements[37], as opposed to least-squares methods which require a minimum of $2L$. With block-wise processing, the reduction in available data samples for channel estimation motivates the use of sparse channel estimation techniques.

The suboptimal detector in Fig. 3.1 is designed to decode each user in succession rather than jointly as in the optimal detector [1]. However, previously decoded information is fed back to improve the decoding capability for later users in the decoding sequence. With enough iterations, all users potentially can benefit from re-use of previously decoded information. In a previous study [36], SIC was applied after multichannel combining in order to remove MAI temporally prior to equalization and decoding. In the current investigation, the application of SIC is considered prior to multichannel combining, while ATR plays the role of spatial crosstalk minimization and multichannel combining. As shown in Fig. 3.1, SIC provides temporal MAI mitigation prior to multichannel combining, such that channel estimates can be formed at the multichannel level by the MP algorithm. Similar to other SIC architectures, iterating the entire process can jointly increase the accuracy of both symbol and channel estimates, potentially enhancing the output signal-to-interference-plus-noise ratio (SINR) for all users.

Following SIC and sparse channel estimation, ATR can be employed to achieve spatial and temporal focusing while simultaneously suppressing residual MAI. ATR was developed as a means of nulling crosstalk between users while maintaining the beneficial qualities of its conventional counterpart [2]. Defining the column vector $\mathbf{d}_k$ as the collection of channel responses in the frequency domain between a user k to an M-element array during the current decoding block,

$$\mathbf{d}_k = \left[\; H_1^k(f) \; \cdots \; H_M^k(f) \; \right]^T \tag{3.1}$$

the filter response at frequency f for focusing the array on user k is given by $\tilde{\mathbf{w}}_k$, the solution to the problem

$$\text{minimize} \quad \mathbf{w}^H \mathbf{R} \mathbf{w} \tag{3.2}$$

$$\text{subject to} \quad \mathbf{d}_k^H \mathbf{w} = 1, \tag{3.3}$$

where the superscript H denotes complex-conjugate transpose. $\mathbf{R}$ is an outer-product matrix,

$$\mathbf{R} = \sum_j P_j \cdot \mathbf{d}_j \mathbf{d}_j^H + \sigma^2 \mathbf{I}, \tag{3.4}$$

designed to emulate the cross-spectral density matrix for an appropriate choice of the regularization parameter σ^2. P_j denotes the power transmitted by user j in the band of interest. This is a quadratic program, and analysis of its dual problem yields the optimal and analytic solution,

$$\tilde{\mathbf{w}}_k = \frac{\mathbf{R}^{-1}\mathbf{d}_k}{\mathbf{d}_k^H \mathbf{R}^{-1} \mathbf{d}_k}, \tag{3.5}$$

which is feasible for all $\mathbf{R} \succ 0$. The optimal weights are calculated for all frequencies in the transmission band, transformed to the time domain, and time-reversed (or phase-conjugated), yielding the set of adaptive time-domain filter coefficients $\left\{ w_1^k(-t) \ \cdots \ w_M^k(-t) \right\}$, as shown in Fig. 1b. Furthermore, we note that for feasible solutions, the optimal value ${\tilde{\mathbf{w}}_k}^H \mathbf{R} \tilde{\mathbf{w}}_k$ represents the interference plus noise experienced by user k at frequency f, and is a suitable metric for ordering the users in SIC.

Although the application of both SIC and ATR may seem redundant from the perspective of MAI removal, they are indeed complementary. SIC and MP can produce channel estimates at the multichannel level as the process iterates and symbol information improves, while ATR cannot, as element-wise channel information is lost when signals are combined across an array. In turn, ATR can suppress residual MAI, minimizing the effect of error propagation between iterations as well as providing the spatial and temporal focusing benefits of conventional time-reversal. To illustrate ATR's mitigation of residual interference, we let $r_i^-(t)$ represent the post-SIC signal out of the i^{th} receiver element,

$$r_i^-(t) = h_i^k(t) * s_k(t) + \sum_{j \neq k} h_i^j(t) * e_j(t), \tag{3.6}$$

assuming the availability of accurate channel estimates (i.e. $\hat{h}_i^j = h_i^j$) and ignoring the effects of noise and transmit power imbalance. Here, $h_i^j(t)$ represents the channel experienced by the j^{th} user to the i^{th} receiver during the current decoding block, and $e_j(t)$ represents the error signal,

$$e_j(t) = s_j(t) - \hat{s}_j(t), \tag{3.7}$$

where $\hat{s}_j(t)$ is the best available estimate of the transmitted signal from user j. The first component of (3.6) represents the desired portion of the received signal after temporal interference cancellation, while the second component of (3.6) represents the residual interference. Because ATR is designed as a spatial interference suppressor, it minimizes any signal component (i.e. $e_j(t)$) distorted by $h_i^j(t)$ for all $j \neq k$ and is therefore capable of suppressing the residual interference following SIC.

3.3 Experimental results from a time-varying channel

To illustrate its performance in a time-varying ocean environment, the proposed receiver is applied to communications data collected during the Kauai Acomms MURI 2011 (KAM11) experiment. The KAM11 experiment was conducted off of the west coast of Kauai in a 100-m deep downward refracting environment (in the same location as KAM08 [21]). In similar fashion to the KAM08 experiment, the KAM11 experiment sought to further investigate the effect of environmental fluctuations on the performance of acoustic communication systems but with an increased focus on multiuser applications. During multiuser transmissions over the 20-30 kHz band, the temporal dynamics of the environment

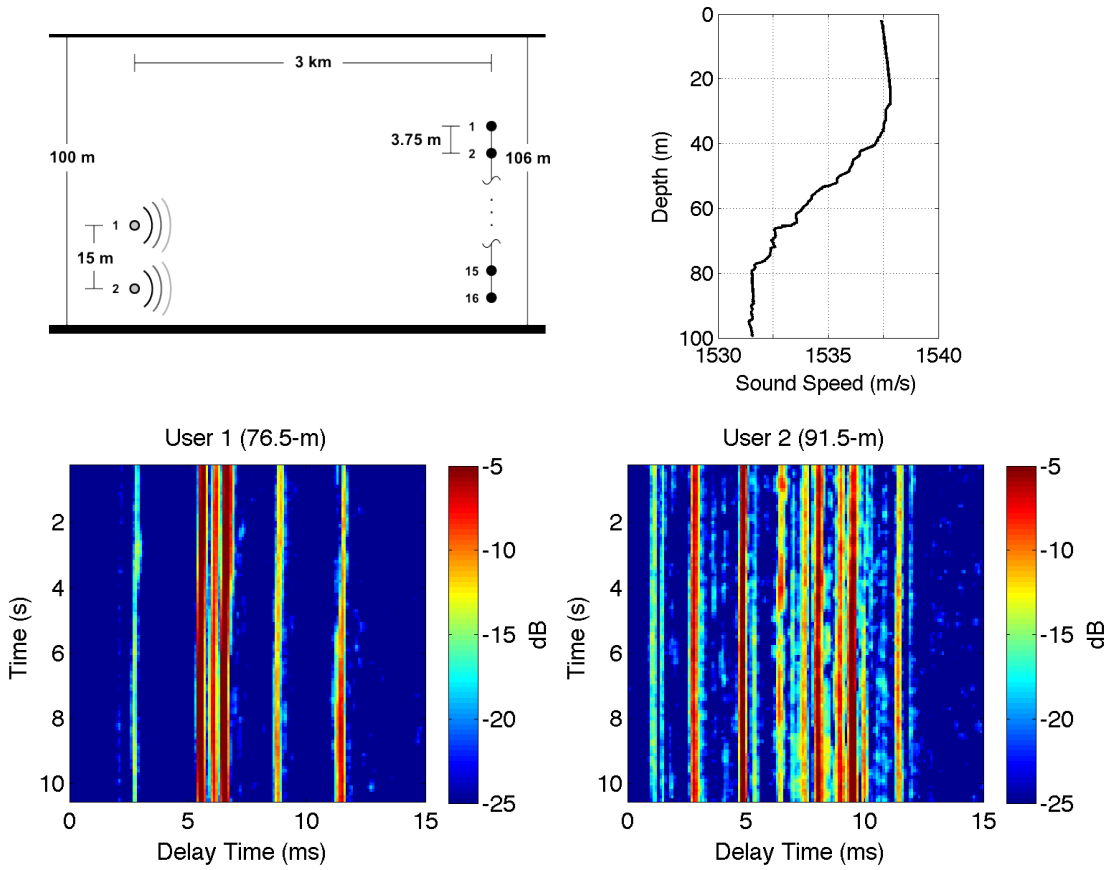

Figure 3.2: KAM11 experiment configuration and environmental conditions: (top) diagram of the KAM11 experiment in which two users transmit to a 16-element receiving array in 100-m deep water and an example sound speed profile collected during the experiment illustrating the downward refracting environment; (bottom) example channel impulse responses between user 1 (left) and user 2 (right) and a single element at 74-m depth of the receiving array taken from the output of MP during single-user processing.

provided a time-varying, rich multipath channel resolvable by the communications receivers. The particular experimental setup used for the data of interest is depicted in Fig. 3.2 along with a sound speed profile and example channel impulse responses measured during the experiment. Two users, labeled users 1 and 2 at depths of 76.5-m and 91.5-m, respectively, transmitted to a vertical receiving array with 3.75-m spacing suspended in 100-m water depth at a range of approximately 3-km. The 10.5-s packets for each user were constructed from independent data modulated with QPSK (user 1) and modified 8-QAM symbols (user 2) and transmitted at a rate of 5 ksps both sequentially (in a single-user setting without MAI) and simultaneously (in a multiuser setting with MAI) from the users under similar channel conditions. With the users transmitting sequentially, their throughput was 10 kbps and 15 kbps, respectively, for a time average of 12.5 kbps (10 kbps and 15 kbps over two packet intervals). With the users transmitting simultaneously, their combined throughput was 25 kbps (10 kbps and 15 kbps over one packet interval).

3.3.1 Single-user communications

Single-user receptions of the packets collected under similar channel conditions as the multiuser packet were considered for this analysis for two main reasons. Perhaps most importantly, it provided a baseline comparison of results between multiuser and single-user decoding performances, which is discussed later. Additionally, the channel variability experienced by each user could be assessed without the impact of MAI. An estimate of the magnitude of the channel impulse response experience by each user (in the absence of MAI) to a single element of the receiving array is presented in Fig. 3.3. Although the arrival structure of the channels remain largely unchanged, the individual paths undergo non-uniform fades, requiring the receiver to adaptively track the time-varying channel.

First, when the packets were processed separately, the block-by-block processor consisted of MP and CTR without SIC nor iterative processing (neither are necessary in the absence of MAI). The results from decoding the single-user packets are presented in Fig. 3.3a. The packets were decoded with output SNRs of 19.3 and 16.7 dB, respectively. As stated previously, these benchmarks provided a

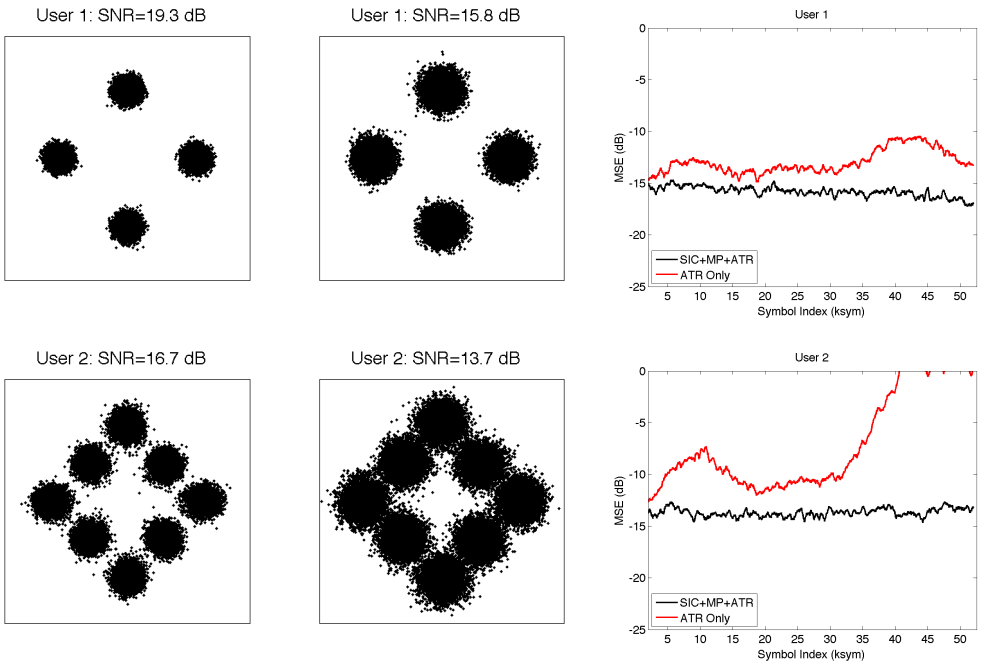

(a) (b) (c)

Figure 3.3: Decoding performance for user 1 (top row) and user 2 (bottom row) from data collected during KAM11: (a) soft symbol estimates from decoding the packets in a single-user setting, (b) final soft symbol estimates after 4 iterations of the combined receiver from decoding the multiuser packet, (c) mean-squared error comparison between the ATR only receiver [2] (without channel updates) and the proposed receiver.

performance ceiling for the analysis of the multiuser packet that follows.

3.3.2 Multiuser communications

Next, the multiuser packet was decoded with block-by-block processing and 4 iterations of the combined receiver depicted in Fig. 3.1. The "Decoder" and "Re-encoder" blocks in Fig. 3.1, which represent the decoding and encoding blocks of an error-correcting code, were omitted to ensure all quoted performance measures did not reflect coding gains. Instead, quantized symbol estimates were directly fed back into the system. With 4 iterations of the proposed receiver, the combined receiver effectively separated the users with output SNRs of 15.8 and 13.7 dB, respectively, as seen in Fig. 3.3b. The degradation from single-user decoding was approximately 3-3.5 dB, which is in agreement with previous results from time-invariant channels [2]. A comparison with the ATR only receiver [2] (without channel updates) was also conducted and is presented in Fig. 3.3c for both users. With the ATR only receiver, the output error slowly grew as the quality of the original channel estimates faded, while the proposed receiver was able to provide accurate channel updates to the combiner. One assumption that was necessary was the availability of an initial channel impulse response between each user and the receiver, a typical assumption necessary for TR communications. For this data, the initial channel estimates were extracted from correlated receptions of simultaneously transmitted Kasami sequences prepended to the multiuser data. However, for a fully asynchronous multiuser system, this assumption must be relaxed, and a channel estimation scheme in the presence of asynchronous MAI must be considered.

3.4 Summary and conclusions

The dispersive underwater acoustic channel has been shown to be able to support multiple users (without an explicit division scheme), increasing the average total system throughput *linearly* in the number of users. It has been shown that through iterative processing of a combined ATR-SIC receiver with intelligent

information re-use, a suboptimal, greedy detector can still achieve multiuser separation in a time-varying channel. For the example presented in this letter, the average system throughput was doubled successfully from 12.5 kbps for single-user transmissions, to 25 kbps with simultaneous multiuser transmissions without a drastic loss in performance – a loss of only about 3-3.5 dB from the single-user baseline which was consistent with previous results.

Acknowledgments

This work was supported by the Office of Naval Research under grants N00014-07-1-0739.

Chapter 3, in full, is a reprint of the material as it appears in "Multiuser Interference Cancellation in Time-Varying Channels, S. E. Cho, H. C. Song, and W. S. Hodgkiss, *Journal of the Acoustical Society of America*, Vol. 131, No. 2, January 2012, pp. EL163–EL169. The dissertation author was the primary investigator and author of this paper.

Chapter 4

Asynchronous Multiuser Underwater Acoustic Communications

An asynchronous multiuser system is proposed to support multple-access underwater communications without the use of code-division multiple-access or a feedback channel. The rich multipath channels experienced by spatially separated users will be sufficient to ensure separation of collided packets at the base station. The iterative receiver will employ a combination of adaptive time-reversal processing, matching pursuit, and successive interference cancellation in a block-wise fashion to achieve multiuser separability. Data collected during the KAM11 experiment is used to illustrate the system's capability in a dynamic, time-varying environment.

4.1 Introduction

Recent research in the field of acoustic communications through shallow water channels has focused on scenarios in which multiple sources are used to transmit acoustically to a single receiving base station, typically to a multi-element receiving array. Although system designs employing multiple sources are inherently more complicated, the potential benefits have been shown in some cases to far outweigh

these complexities. Currently, there are two main categories of multiple source system designs, one in which the sources belong to a single user and transmit in unison and one in which each of the sources belong to a separate user and transmit independently from one another. In the first category, typically known as single-user multiple-input, multiple-output (MIMO) communications, the additional transmitters can be used in conjunction with space-time block codes to increase either the robustness or throughput in transmission (or a tradeoff in between).[26] The focus of this letter is the second category, referred to as multiple-access or multiuser communications, which allows spatially separated users to simultaneously transmit independent messages to a shared base station. If constructed properly, multiple-access systems can deliver both substantial throughput gains (versus single-user systems) and alleviate networking burdens in multiuser systems.

One of the primary benefits of multiple-access systems is the linear increase in total throughput that is possible over single-user systems. Some of the earliest work in multiuser underwater acoustic communications included the extension of the adaptive decision-feedback equalizer (DFE) to multiple-access channels[1]. Since then, alternative methods based on time-reversal (TR) techniques also have been investigated[2]. These promising results showed that with careful design of the receiver architecture, the rich multipath channels common in shallow water environments opened opportunities for multiple-access communications without the need for spreading codes (i.e. CDMA), which necessarily sacrifice throughput to ensure multiuser separability at the detectors[15, 16]. The TR work relied on the premise that in rich multipath environments, spatially separated users (sometimes by only a few meters) could observe channel impulse responses (CIRs) to the base station (typically kilometers away) that were different from one another (e.g., see Fig. 4.3). With reliable estimates of these CIRs and assumptions of time-invariance of the channel, the receiver could leverage these differences to achieve multiuser separability. Further work demonstrated that the coupling of TR techniques with successive interference cancellation (SIC) and iterative processing yielded a receiver capable of achieving separation even in time-varying environments[38] (or in the context of MIMO)[24].

However, the previous TR work required some synchronization amongst the users. In TR communications, an initial estimate of the CIR from each of the users was required at the base station before decoding of data bearing signals could commence, and was obtained through receptions of channel probes from each of the users in the absence of multiple-access interference (MAI). This MAI-free condition implied that the transmission of channel probes by users was organized into time slots by the base station through a reliable feedback channel (from the base station to the user). This scenario would require significant networking overhead and would be unfavorable in the underwater acoustic channel, where the combination of small coherence times (typically much less than a second) and large propagation delays (typically much more than a second) discourage the reliance on feedback and two-way communications.

The focus of this letter is to demonstrate that even when users transmit asynchronously through a time-varying channel, reliable channel estimates can be obtained and multiuser separation achieved with the combination of TR processing and SIC. Furthermore, when coupled with matching pursuit (MP) and iterative processing, the resulting architecture can maintain separation even in time-varying environments. From the users' perspective, this work potentially provides the capability to communicate without the need of a feedback channel from the base station and without the need to cooperate with other users. At the base station, collided packets potentially can be separated, dramatically decreasing the packet error probability without any additional networking overhead, two of the most important factors underpinning popular networking architectures.[39]

4.2 Multiuser System Design

In order to support a small network of asynchronous users, a simple packet-based transmission scheme is employed that utilizes a user-dependent channel probe at the beginning of each user's packet. The receiver, which carries the computational burden in this system, implements a block-by-block processing scheme that switches between two different modes of operation based on the number of

users transmitting within each block.

4.2.1 Transmission Scheme

The data packets transmitted by the users are composed of channel probes followed by sequences of data bearing symbols drawn from a constellation (e.g., see Fig. 4.2). The channel probes at the front of each packet are single periods of Kasami sequences unique to each user. Kasami sequences are specially designed maximum length (ML) sequence typically used in spread spectrum communications because of their MAI mitigation properties[9]. However, it is important to note that in this design, the sequences are used only as channel probes to uniquely identify and obtain an initial CIR estimate from each user but not to "spread" the data bearing portion of the signal to gain MAI suppression. Following the Kasami sequence, the user transmits data as a sequence of symbols drawn from a constellation. Once constructed, a user's packet can be transmitted to the base station at any time, possibly interfering with other users' transmissions.

4.2.2 Asynchronous Multiuser Detection

At the base station, the multichannel received data are demodulated to complex baseband, and the initial detection of transmitting users is performed by matched filtering with the unique Kasami sequence for each potential user. From the output of the matched filters, the receiver can determine which users are active and when their transmissions begin as well as obtain an initial CIR estimate for each of the transmitting users. After this initial processing, the demodulated signal $r_i[n]$ is decoded in block-by-block fashion in one of two receiving modes depending on the number of transmitting users within a given block. For blocks in which only a single active user is transmitting, a single-user receiver with conventional TR and MP[21].

More generally, when a block contains collided packets from different users, a combined adaptive time-reversal (ATR), a TR approach with spatial crosstalk nulling[2], and SIC receiver is implemented to separate the collided packets[38].

The block diagram for a two user receiver is provided in Fig. 4.1, and is easily generalizable for larger numbers of users. The combined ATR and SIC receiver can separate collided packets by removing MAI in two different ways. While decoding one of the users, for example user j, SIC combines the CIR estimates $h^{(k)}[n]$ of interfering users, user k for $k \neq j$, and symbol estimates $\hat{d}_n^k$ (decoded during a previous iteration) to suppress MAI at the multichannel level. Similar to other TR receivers, this multiuser detector uses $h^{(j)}[n]$, its CIR estimate for the desired user, for multichannel combining and ISI mitigation. However, the ATR combiner implemented here also mitigates MAI by utilizing its knowledge of the other users' CIRs. Following the ATR combiner, a DFE specific to user j with feedforward and feedback filters $a^{(j)}[n]$ and $b^{(j)}[n]$ is used in conjunction with an embedded phased lock loop to compensate for residual ISI and a time-varying phase rotation θ_j. It should be noted that during the first decoding iteration, symbol estimates from competing users are not available to the receiver, and SIC cannot be performed. Thus, during the first iteration, ATR is the sole source of MAI mitigation.

Once symbol estimates $\hat{d}_n^j$ are available to the receiver, they are used in conjunction with the mitigated MAI signals at the output of SIC, to update the receiver's estimate of the CIR $h_i^{(j)}[n]$ for each receiving element i. These new estimates, illustrated with dotted lines in Fig. 4.1, are utilized by the receiver during further iterative processing of the current block and in the next block to initialize the ATR combiner. Block-wise procesing and the MP algorithm provide this receiver with the capability to track each user's time-varying channel for the duration of their packets.

4.3 KAM11: Receiver Analysis

The Kauai Acomms MURI 2011 (KAM11) experiment was a multi-university research initiative focused on studying the impact of environmental fluctuations on underwater acoustic communication systems. Similar to the KAM08 experiment, the KAM11 experiment was conducted off of the west coast of Kauai in a roughly 100-m downward refracting environment. For the purposes of this

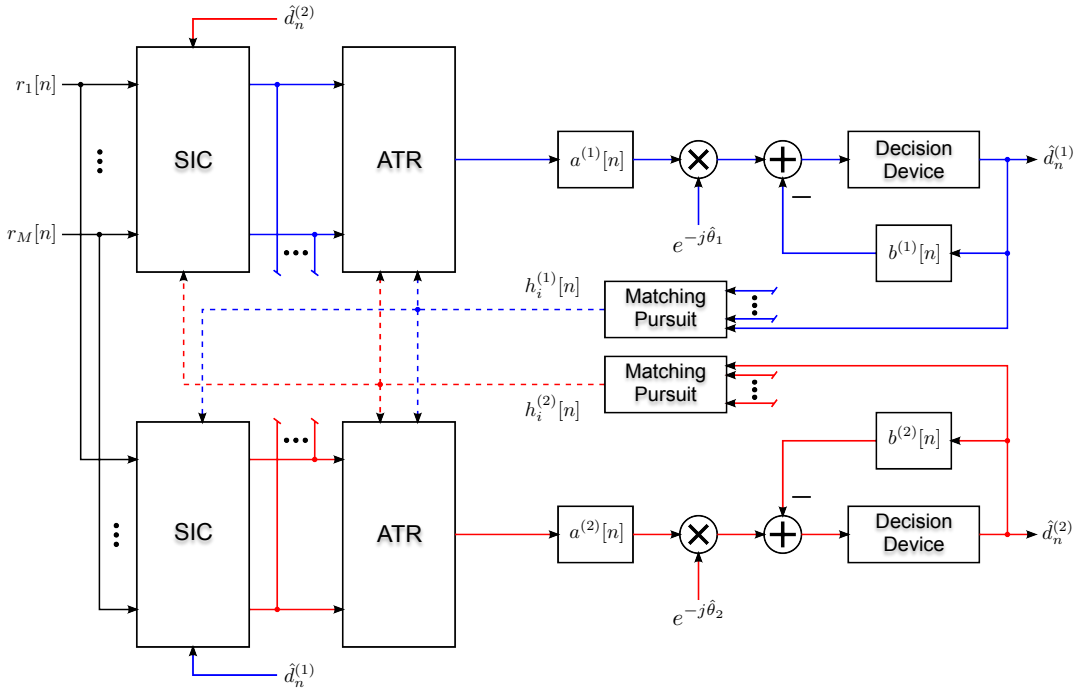

Figure 4.1: (Color online) Receiver block diagram employing SIC, ATR, MP, and a joint PLL/DFE for separating collided multiuser packets. After the first iteration, the receiver re-uses symbol estimates $\hat{d}_n^{(1)}$ and $\hat{d}_n^{(2)}$ for channel updates (shown in dotted lines) and to obtain an estimate of the MAI created by each user, which is removed by the SIC algorithm to improve the decoding performance during further iterations.

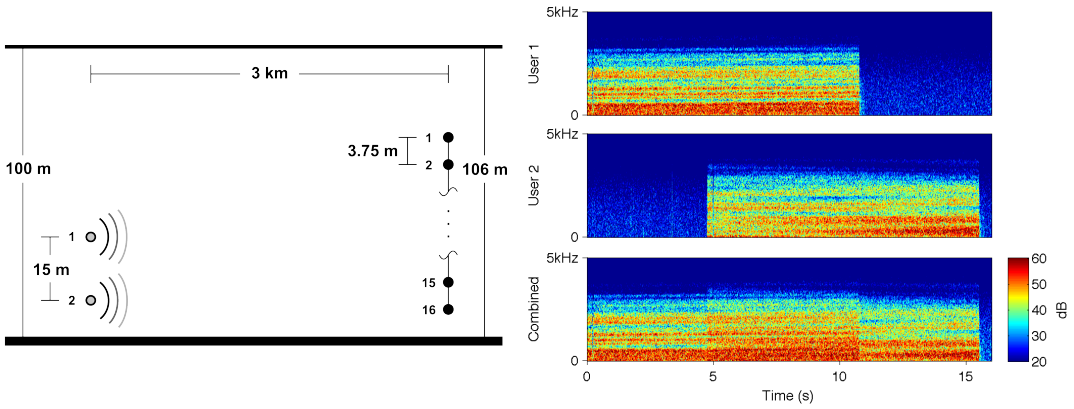

(a) (b)

Figure 4.2: (Color online) (*a*) Diagram of the KAM11 experiment in which two users transmit to a receiving array 3 km away through a 100-m deep channel; (*b*) spectrograms illustrating the creation of a synthetic, asynchronous multiuser packet at Element 4 of the receiving array in complex baseband: (*top*) recorded packet from User 1, (*middle*) recorded packet from User 2 delayed by about 5 seconds, (*bottom*) combined multiuser packet used for decoding.

letter, data were collected during the experiment on a 16 element receiving array from two independent sources separated vertically by about 15-m while transmitting over the 20-30 kHz frequency band at a range of approximately 3 km. A diagram of the experiment is provided in Fig. 4.2. More information about the KAM08 and KAM11 experiments is available in the literature[21, 38].

To create an asynchronous packet, independent transmissions from each of the sources (denoted User 1 and User 2) were recorded by the array and added together in post-processing (transmissions JD186 03:40 UTC and JD186 05:40 UTC, respectively). As shown in Fig. 4.2, an arbitrarily chosen delay of roughly 5 seconds was introduced for User 2 with respect to User 1. Each user transmitted a 1023 length (roughly 200 ms) Kasami sequence as a channel probe followed by a 10.5-s packet of symbols drawn from constellations, 16-QAM from User 1 and a modified 8-QAM from User 2, at a rate of 5000 symbols per second. In the combined packet, User 2 experienced a signal-to-interference ratio (SIR) of roughly

-2.5 dB indicating it to be the weaker user between the two. From Fig. 4.2 it is apparent that User 2 also experiences a CIR that varies more severely than User 1 and a received SNR that increases as its transmission progresses.

A summary of the receiver's performance when applied to the example asynchronous packet is shown in Fig. 4.3. First, the receiver detected and obtained an initial CIR estimate by processing the Kasami channel probes from the users. The initial CIR estimates are shown in the top panels of Fig. 4.3. It should be noted that although the initial CIR estimate for User 1 was estimated without MAI, the initial estimate for User 2 was obtained successfully from received data in the presence of strong MAI (SIR of -2.5 dB). In this case, the channel probe was designed to be of sufficient length to provide enough coding gain to overcome strong MAI. As the initial CIR estimation process is critical to the performance of the receiver, a longer Kasami sequence could be used to further ensure robust estimation of the initial CIR from all users.

Once initial CIR estimates were available, the receiver began block-wise processing of the collided packet with a block size of 0.5 sec or 2500 symbol periods. A portion of the preceding block was reprocessed with the current block to minimize any potential boundary effects. Both sets of feedforward and feedback filters were tracked with recursive least-squares algorithms and forgetting factors of 0.998. Additionally, the proportional and integral PLL tracking constants were set to 1×10^{-4} and 1×10^{-5}, respectively. For blocks in the first and last 5 seconds of the combined packet in which no MAI was present (see Fig. 4.2), the single-user receiver discussed previously was used to decode the blocks with combined output SNRs of roughly 19.5 dB and 20.3 dB for Users 1 and 2, respectively. For the blocks in the middle 5 seconds of the combined packet in which the two users' transmissions collided, four iterations of the multiuser receiver were required to achieve multiuser separation and led to output SNRs of roughly 16.7 dB and 14.0 dB, respectively. With four iterations of processing the receiver was able to perform accurate channel updates and combine these estimates with symbol estimates from previous iterations to remove MAI in similar fashion to previous SIC receivers[38]. A roughly 3 dB performance decline between single and multiuser performances

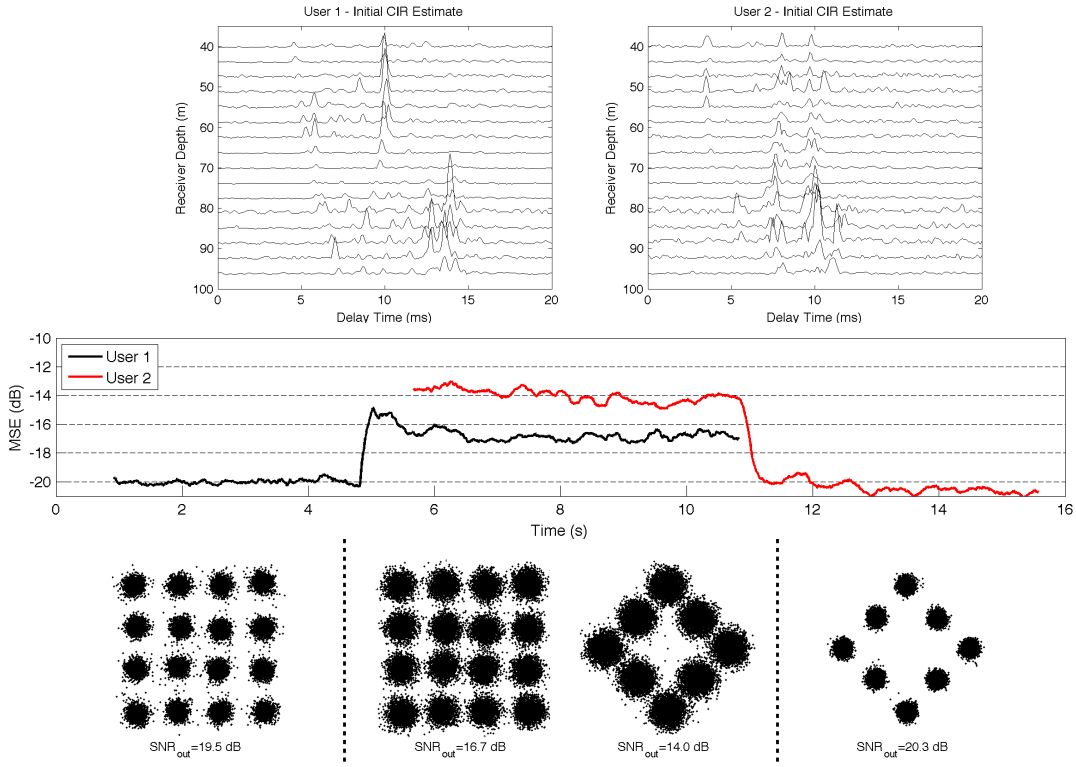

Figure 4.3: (Color online) Performance of the proposed multiuser receiver on data from the KAM11 experiment: (*(top)* initial CIR estimates for User 1 (estimated without MAI) and User 2 (estimated with a SIR of about -2.5 dB); (*middle*) mean-squared error of symbols estimates for both users (excluding symbols used in training); (*bottom*) aggregate soft symbol estimates for the portions of the packet when each user is decoded without MAI (*outter panels*) and with MAI (*inner panels*).

has been observed in previous work[38, 2], and is experienced by User 1 in this example as well. However, the decline for User 2 is larger than expected at roughly 6 dB but seems to be due to the increased received SNR for User 2's transmission toward the latter half of the packet as illustrated in Fig. 4.2. The mean-squared error of soft symbol estimates taken during the final iteration of decoding as well as scatter plots of these estimates are shown in the middle and bottom panels of Fig. 4.3, respectively, and illustrate clearly the performance decline when blocks contain collided packets from the two users. However, the scatter plots, which are segmented into portions of packets decoded within (inner panels) and without (outer panels) MAI, show that the receiver is still able to decode the symbols successfully and separate the two packets.

One challenge of the underwater acoustic multiple-access channel that must be considered and overcome by all systems is the near-far problem which characterizes the potentially imbalanced received SNR between competing users at the base station. Spatially separated users may have received SNRs that may be imbalanced perhaps because some of the users may be in a deep fading region of the environment or simply because some of the users may be farther away from the base station. Nonetheless, multiple-access system designs that can overcome the near-far problem are certainly more favorable than those that cannot. In this regard, the proposed asynchronous receiver's applicability to the near-far problem were considered by scaling the contribution to the asynchronous packet from just one of the users (User 1) effectively shifting the input SIR with respect to the other user. The results presented in Fig. 4.4 illustrate that successful decoding and multiuser separability is achievable with this receiver even as the input SIR is shifted several dB.

4.4 Summary and Conclusion

A system was developed to support asynchronous multiuser communications through a time-varying channel, providing multiuser separability at the base station without CDMA or a feedback channel. Although the users would utilize

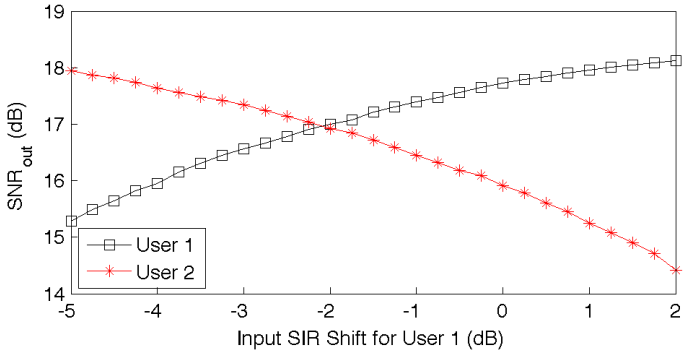

Figure 4.4: (Color online) Performance of the multiuser receiver as the received data from User 1 is scaled to shift the signal-to-interference ratio experienced with respect to User 2. The output SNR values are computed from mean-squared symbol errors aggregated over both single and multiuser portions of the users' decoded packets. The plots appear asymmetric about 0 dB because User 1 experiences a SIR of approximately 2.5 dB in the original data.

the same bandwidth at the same time, CDMA was found to be unnecessary in underwater acoustic channels where the rich multipath channels experienced by spatially separated users was sufficient to separate collided packets at the base station. With a base station employing block-wise processing of a TR receiver coupled with iterative SIC for the blocks containing interference, the receiver was found to be capable of providing separation to the users without the need to align them in the frequency or time domains, minimizing the need for feedback to the users. The receiver was applied to data collected during the KAM11 experiment, in which two users transmitted asynchronously across a 3 km channel to a 16-element vertical array deployed in 100-m deep water. Their packets consisted of Kasami probes followed by 10.5-s of QAM symbols and were transmitted asynchronously to the base station. The proposed receiver was able to separate the collided portions of the packets even as a simulated near-far problem was introduced to negatively impact the system.

Acknowledgements

This work was supported by the Office of Naval Research under grant N00014-07-1-0739.

Chapter 4, in full, is a reprint of the material as it appears in "Asynchronous Multiuser Underwater Acoustic Communications, S. E. Cho, H. C. Song, and W. S. Hodgkiss, *Journal of the Acoustical Society of America*, in press, 2012. The dissertation author was the primary investigator and author of this paper.

Chapter 5

Multiuser Acoustic Communications with Mobile Users

A multiuser receiver is developed capable of separating receptions from independent, mobile users whose transmissions overlap in both time and frequency. With respect to any one user's Doppler corrected signal, the other communication signals appear as multiple-access interference distributed across the Doppler dimension. A receiver composed of an adaptive time-reversal processor embedded within a successive interference cancellation framework previously was developed for systems that are limited to stationary users. This paper extends the receiver to properly remove the interference from moving sources. The combined receiver's strength is the ability to remove interference in both the temporal and spatial domains, and this property is shown to be preserved even when users are in motion. When applied to data collected during a recent shallow water experiment (KAM11), the receiver is shown to be capable of separating packets in a two user system where one user is moving while the other is stationary.

5.1 Introduction

Multiple-input multiple-output (MIMO) communications has been the subject of increased attention for acoustic communication applications through shallow water channels.[22, 26, 40, 24, 41] The MIMO systems provide a system designer with much more design flexibility over single-input, single-output (SISO) systems. With the addition of a few transmitters and receivers, the system can utilize the increased number of channels (one for each transmitter/receiver pair) in a variety different ways. The tradeoff typically is characterized as a diversity gain (or robustness) versus multiplexing gain (increased throughput). On one extreme, the uniqueness amongst the channel impulse responses (CIRs), can be used to transmit the same information over different channels, minimizing the probability of poor reception (i.e. the chance that all communications channels are poor). However, the multiple CIRs also can be utilized to transmit independent information simultaneously, potentially achieving a large multiplexing gain. Approaches utilizing space-time block codes allow the designer efficiently to make a trade off between these two extremes.[26] Towards the end of higher throughput lies the field of multiple-access or multiuser underwater acoustic communications, where the multiple transmitters are assumed each to belong to an independent user separated in space. With each user transmitting simultaneously, the uniqueness between the users' sets of CIRs allows their information to be separated at the base station, typically a receiving array.

One popular approach to multiple-access communications in shallow water channels is code-division multiple access (CDMA), a design that originated in the wireless community where each user is assigned a finite-length code used to "spread" their narrowband signal to occupy the total available bandwidth.[15, 16] At the receiver, the signal is "de-spread" with the same code (through convolution), which simultaneously acts to enhance the desired portion of the signal with a coding gain and to suppress the interference caused by other users in the system. Although CDMA is a popular multiple-access system design, other approaches have been investigated for underwater acoustic communication that do not require the throughput loss resulting from securing interference suppression with code

division. These techniques implicitly rely on the rich multipath environments and spatial diversity common in shallow water channels to provide each user with a unique set of CIRs in place of a unique spreading code. One such approach, known as time-reversal processing, treats the CIRs effectively as spreading codes, and applies a space/time matched-filter (the time-reversed CIRs) effectively to act as a de-spreader achieving spatial focusing.[23] Of course, the CIRs for differing users in general are not orthogonal and do not provide any bound on the amount of multiple-access interference (MAI) that passes through the convolution at the receiver (as in CDMA). Therefore, the MAI must be dealt with accordingly.[36, 2, 24]

A recent investigation embedded an adaptive time-reversal (ATR) processor, a design where the receiver's matched-filter is designed to suppress interference in the spatial domain, within an iterative successive interference cancellation (SIC) framework.[38] The SIC process estimated and removed interference along the temporal dimension, and the combination with ATR was shown to be an effective means of minimizing MAI. With the addition of matching pursuit (MP), a sparse channel estimation algorithm,[35] the overall receiver was applied successfully to data with stationary users in a time-varying environment. This paper considers the more general situation with users in motion, where the effect of Doppler must be considered. In such cases, the multiuser signals may be distributed across the Doppler dimension, and separation becomes a non-trivial task. When decoding any one user's Doppler corrected signal, the MAI removal process must incorporate the impact of Doppler correction on the MAI prior to cancellation.

The rest of this paper will introduce a receiver capable of separating packets from multiple independent, and potentially moving, sources. In Section 5.2, a channel model will be developed that incorporates transmissions from independent sources at potentially different mean Doppler shifts. In Section 5.3, a receiver will be presented that can achieve multiuser separation through multiple iterations of an ATR processor embedded within a SIC framework with MAI modeled and removed at different Doppler shifts. In Section 5.4, results from applying the receiver to data collected during a shallow water experiment will be presented.

5.2 Multiuser Signal Model

A model for the received signal is developed that incorporates transmissions from independent users communicating to a central receiving array potentially at the same time and over the same frequency band. The model is limited to users in the far field where the acoustic propagation is characterized as approximately horizontal propagation through a waveguide. The CIR between each of the users and the receiver is assumed to be time-varying. Furthermore, because each of the users potentially are in motion, the received signal is modeled as being a combination of their signals but with each user's transmission distorted by an independent Doppler shift (more generally, an independent dilation or compression).

5.2.1 Passband Model

To begin the derivation, $x(t)$ is defined as the complex-valued information signal (i.e. pulse-shaped QAM symbols) constructed in baseband. When transmitted at a carrier frequency of f_c, this signal uniquely determines the passband signal $x_{\text{pb}}(t)$ through the relationship

$$x_{\text{pb}}(t) = \sqrt{2}\text{Re}\left\{x(t)e^{j2\pi f_c t}\right\}. \tag{5.1}$$

$x(t)$ is also commonly referred to as the complex envelope of $x_{\text{pb}}(t)$ and requires that the bandwidth W of the signal be sufficiently small, i.e. $\frac{W}{2} < f_c$. The factor of $\sqrt{2}$ is a normalization constant that ensures the energies of $x_{\text{pb}}(t)$ and $x(t)$ are the same. After interaction with a time-varying multipath channel, the signal is observed at the receiver with additive noise $n_{\text{pb}}(t)$ as

$$r_{\text{pb}}(t) = \sum_{p=1}^{P} a_p(t)x_{\text{pb}}(t - \tau_p(t)) + n_{\text{pb}}(t), \tag{5.2}$$

a superposition of P copies of $x_{\text{pb}}(t)$ each delayed by τ_p according to the length of the propagation path p and scaled by a gain $a_p \in \mathbb{R}$ which accommodates for path loss effects and possible interactions with lossy boundaries. The time dependance of the delays τ_p and gains a_p accounts for changes of the propagation medium (the

ocean) and effects of transmitter and receiver motion. The cumulative effect of the channel can be summarized by the expressing the previous equation as

$$r_{\mathrm{pb}}(t) = \int_{-\infty}^{\infty} \sum_{p=1}^{P} a_p(t)\delta(\tau - \tau_p(t))x_{\mathrm{pb}}(t-\tau)d\tau + n_{\mathrm{pb}}(t) \tag{5.3}$$

$$= h_{\mathrm{pb}}(t,\tau) \star x_{\mathrm{pb}}(t) + n_{\mathrm{pb}}(t), \tag{5.4}$$

where $(\star)$ is the convolution operator, and defining

$$h_{\mathrm{pb}}(t,\tau) = \sum_{p=1}^{P} a_p(t)\delta(\tau - \tau_p(t)) \tag{5.5}$$

as the time-varying CIR, the channel's response at time t due to an impulse applied at time $t-\tau$. Equations (5.4) and (5.5) provide a general model of acoustic communication through time-varying, Doppler spread environments. For the purposes of this work, however, the following simplifications will be made:

- As the users move through the environment, their transmissions experience a Doppler compression or dilation which depends on the propagation path. The differences in the compression or dilation leads to a Doppler spread. The model will be restricted to propagation from the far field, limiting the mobile users to ranges much greater than the water depth. With this assumption, all significant paths will arrive at the receiver with very small angular spread, allowing the Doppler compression or dilation to be assumed to be path independent and modeled by a single Doppler parameter. Accurate estimation and equalization of Doppler spread channels is still an active area of research and requires further investigation[42, 43, 44].

- The rate of channel fluctuations will be restricted. These fluctuations are caused by physical changes in the medium, e.g. surface waves, internal waves, etc., that change at relatively modest time scales (seconds or longer). The receivers discussed in Section III will utilize block-based processing with relatively small block lengths (50 ms), allowing the physical properties of the channel to be assumed constant for the duration of the block.

The first simplification will isolate transmitter and receiver motion as the dominant source of time-variations of the arrival times $\tau_p(t)$. Steady transmitter and receiver motion changes the propagation distance along path p (here, approximated as horizontal paths), denoted $R_p(t)$, by

$$R_p(t) = R_p(0) + v_p t, \tag{5.6}$$

where v_p is the radial component of the transmitter velocity as observed by the receiver along path p, and $R_p(0)$ is the initial path length at time $t = 0$. Positive values of v_p denote motion away from the receiver while negative values denote motion towards the receiver. This manifests as time-varying arrival times of the form

$$\tau_p(t) = \frac{R_p(0)}{c} + \frac{v_p}{c} t \tag{5.7}$$

$$= \tau_p^{(0)} + \frac{v_p}{c} t, \tag{5.8}$$

where $\tau_p^{(0)}$ is the initial path delay at time $t = 0$, and c is the speed of sound in water (about 1500 m/s). From (5.2), this yields a received signal of

$$r_{\text{pb}}(t) = \sum_{p=1}^{P} a_p(t) x_{\text{pb}} \left(t - \tau_p^{(0)} - \frac{v_p}{c} t \right) + n_{\text{pb}}(t) \tag{5.9}$$

$$= \sum_{p=1}^{P} a_p(t) x_{\text{pb}} \left(\lambda_p (t - \tau_p') \right) + n_{\text{pb}}(t), \tag{5.10}$$

after defining $\lambda_p = 1 - v_p/c$ as the Doppler coefficient along path p and a change of variables $\tau_p' = \tau_p^{(0)}/\lambda_p$. The Doppler effect compresses or dilates the communications signal, and the severity of compression or dilation depends on the rate of change of the arrival time of path p, or $\frac{\partial}{\partial t}\tau_p(t)$. The differences in λ_p lead to Doppler spread, but at ranges much greater than the water depth (i.e. the far field), significant paths arrive at similar low grazing angles resulting in a small Doppler spread. Thus, with minimal loss of generality, we assume all paths share a common Doppler coefficient, the mean Doppler shift λ, giving a received signal model of

$$r_{\text{pb}}(t) \approx \sum_{p=1}^{P} a_p(t) x_{\text{pb}} \left(\lambda (t - \tau_p') \right) + n_{\text{pb}}(t). \tag{5.11}$$

Although the derivation began with a channel constructed with time-varying path delays, under the assumptions made, the final passband model represents the received signal as a superposition of scaled and delayed copies of $x_{\text{pb}}(t)$ compressed or dilated by only a single Doppler parameter λ. In other words, (5.11) also can be expressed as

$$r_{\text{pb}}(t) = h_{\text{pb}}(t,\tau) \star x_{\text{pb}}(\lambda t) + n_{\text{pb}}(t), \tag{5.12}$$

where

$$h_{\text{pb}}(t,\tau) = \sum_{p=1}^{P} a_p(t)\delta(\tau - \tau'_p) \tag{5.13}$$

is also a time-varying CIR, but the path delays τ'_p remain constant with time. Effectively, the time-varying component of the path delays that is common among all paths can be viewed as a compression or dilation of the signal at the transmitter itself.

5.2.2 Baseband Model

Substituting the complex baseband representations of $r_{\text{pb}}(t)$, $x_{\text{pb}}(t)$, and $n_{\text{pb}}(t)$ into (5.11) gives

$$\begin{aligned}
&\text{Re}\left\{r(t)e^{j2\pi f_c t}\right\} = \\
&\quad = \sum_{p=1}^{P} a_p(t)\text{Re}\left\{x(\lambda(t-\tau'_p))e^{j2\pi f_c \lambda(t-\tau'_p)}\right\} + \text{Re}\left\{n(t)e^{j2\pi f_c t}\right\} \qquad (5.14)\\
&\quad = \text{Re}\left\{\left[\sum_{p=1}^{P} a_p(t)e^{-j2\pi f_c \lambda \tau'_p} x(\lambda(t-\tau'_p))e^{j2\pi f_c(\lambda-1)(t-\tau'_p)} + n(t)\right] e^{j2\pi f_c t}\right\}. \qquad (5.15)
\end{aligned}$$

The complex baseband system model is obtained through the input/output relationship of the baseband signals in (5.15), or

$$r(t) = \sum_{p=1}^{P} a'_p(t)x(\lambda(t-\tau'_p))e^{j2\pi f_c(\lambda-1)(t-\tau'_p)} + n(t), \tag{5.16}$$

where the time-invariant phase rotation of $-2\pi f_c \lambda \tau'_p$ has been incorporated into model by redefining the path gains as the complex-valued quantities $a'_p(t) =$

$a_p(t)e^{-j2\pi f_c\lambda\tau'_p}$. The baseband model equivalently can be expressed as

$$r(t) = h(t,\tau) \star x(\lambda t)e^{j2\pi f_c(\lambda-1)t} + n(t), \tag{5.17}$$

where $h(t,\tau)$ is defined as the complex-baseband equivalent CIR,

$$h(t,\tau) = \sum_{p=1}^{P} a'_p(t)\delta(\tau - \tau'_p). \tag{5.18}$$

The quantity $f_d = f_c(\lambda - 1)$ is known as the Doppler frequency offset and is measured in Hz. Although the phase rotation from this quantity sufficiently characterizes the Doppler effect in narrowband systems ($W \ll f_c$), wideband systems must also correct the compressed or dilated signal $x(\lambda t)$ with proper resampling.

The baseband model is generalized to multiple independent sources by applying the index k to represent the k^{th} user and a user-dependent transmission delay Δ_k, and to multiple receivers by applying the index i to represent the i^{th} receiver to achieve the baseband system model

$$r_i(t) = \sum_k h_i^k(t,\tau) \star x_k(\lambda_k(t-\Delta_k))e^{j2\pi f_c(\lambda_k-1)(t-\Delta_k)} + n_i(t). \tag{5.19}$$

For notational convenience (5.19) is expressed as

$$r_i(t) = \sum_k h_i^k(t,\tau) \star x_k(\lambda_k t - \Delta_k)e^{j2\pi f_c(\lambda_k-1)t} + n_i(t) \tag{5.20}$$

by incorporating the time-invariant phase rotation of $-2\pi f_c(\lambda_k - 1)\Delta_k$ into the channel $h_i^k(t,\tau)$ and applying a change of variables of $\Delta_k := \Delta_k\lambda_k$.

Because the receiver will employ block-by-block processing, all signals will be assumed to represent components in the block currently being decoded. For example, $r_i(t)$ will be interpreted as the received signal at receiver i for the current block, and $x_k(t)$ the signal transmitted by user k during the current block. With small enough block sizes, $a'_p(t)$, the only time-varying component remaining in $h_i^k(t,\tau)$, safely can be assumed to be time-invariant for the duration of a block. The final baseband signal model

$$r_i(t) = \sum_k h_i^k(t) \star x_k(\lambda_k t - \Delta_k)e^{j2\pi f_c(\lambda_k-1)t} + n_i(t) \tag{5.21}$$

incorporates this change by removing the time-dependence of $h_i^k(t,\tau)$ with the understanding that it is only constant within the block currently being decoded. With channel updates preformed as decoding progresses, the receiver will be able to track the fluctuations of the channel.

5.3 Multiuser Receiver Design

As a multiuser decoder, the goal of the receiver is to retrieve each user's data signal $x_k(t)$ from the overlapping receptions contained in the signal given in (5.21). In earlier work, a receiver was designed to decode all $x_k(t)$'s jointly,[1] but recent work suggests that other receiver designs can achieve multiuser separation while at the same time being computationally efficient.[36] Furthermore, it is unclear whether this earlier work could be extended to mobile users, where the received signal is a composition of signals distorted by independent Doppler shifts.

Recently, an iterative application of a combined SIC and ATR receiver was applied in a block-by-block implementation and shown to be capable of minimizing interference, providing the MP channel estimation algorithm with interference mitigated signals to reestimate the channel.[38] This receiver first was applied to time-invariant channels, then to time-varying channels (without source motion). The focus of this work is the adaptation of this receiver to compensate for sources in motion. Fig. 5.1 illustrates the receiver adapted for sources potentially in motion. An alternative to SIC architectures is parallel interference cancellation (PIC), which has been studied for MIMO communications.[45] Instead of decoding each user's data in succession, PIC decodes them in parallel, but SIC and PIC become similar when multiple iterations are applied.[27]

Before describing the necessary receiver modifications with mobile users in the following sections, the iterative block-by-block processing will be discussed. As shown in the two user example in Fig. 5.2, each block is processed during each iteration as follows:

- Iteration 1 - For the first iteration, updated CIR estimates are not available to the receiver, and thus CIR estimates from the previous block or training

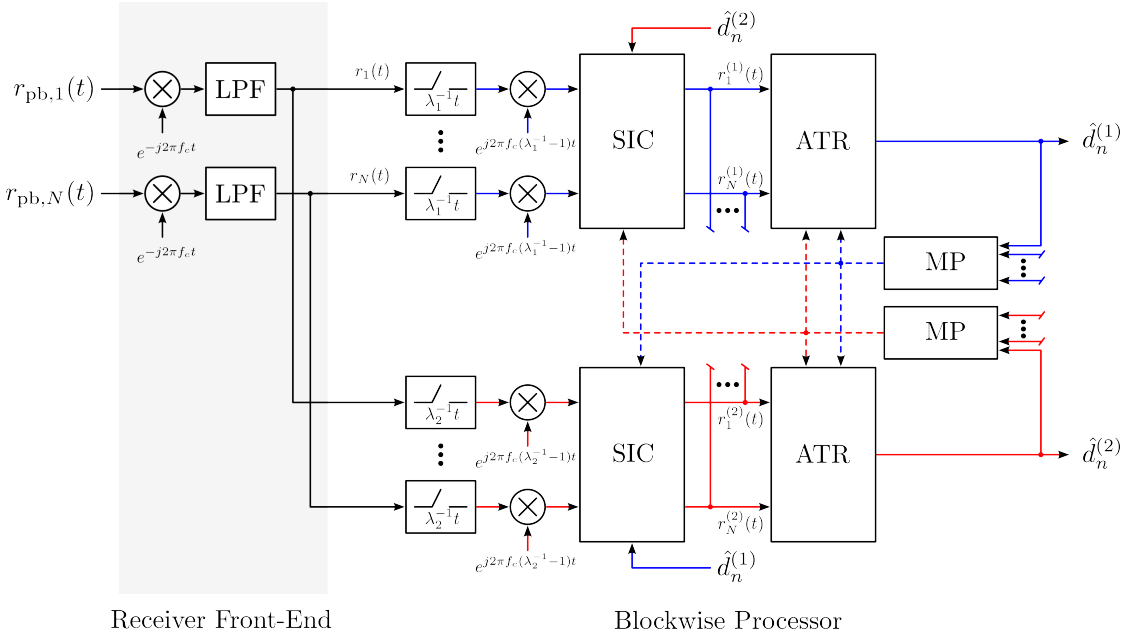

Figure 5.1: (Color online) SIC with embedded ATR and MP for a two user system. Each user is decoded in succession, with interference removed with each iteration. Estimated symbols $\hat{d}_n^{(k)}$ are combined with channel updates to estimate the MAI. SIC applies the proper Doppler correction to the interference before synchronization, scaling, and subtraction.

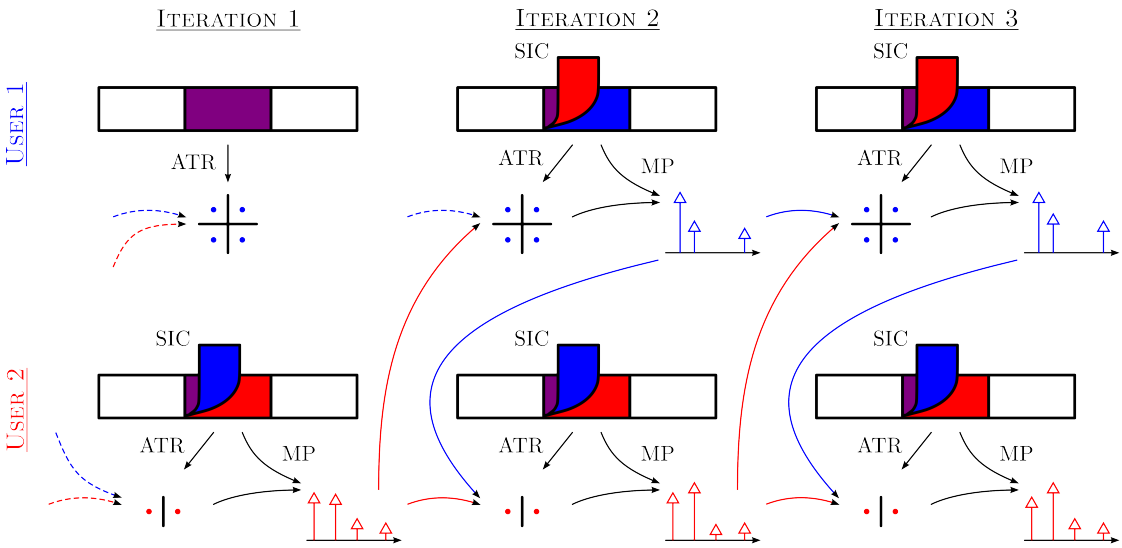

Figure 5.2: (Color online) Illustration of processing a single block with three iterations of the proposed receiver for a system with two users, color-coded blue (User 1) and red (User 2). Dashed colored lines represent channel estimates from the previous block (or estimated during training) while solid colored lines represent channel estimates from the current block. Notional representations of constellations and impulse responses are shown below the block being processed.

are used (dashed lines in Fig. 5.2). First, User 1 is decoded with ATR to produce symbol estimates. Before decoding User 2 with ATR, User 1's symbol estimates are combined with User 1's previous CIR estimate by SIC to remove MAI. User 2's symbols are then decoded and a channel update is performed with MP (solid red lines in Fig. 5.2).

- Iteration 2 - During the second iteration, User 1 is again decoded first, but SIC is able to employ CIR and symbol estimates from User 2 to remove MAI prior to decoding and channel updating with MP.

- Iterations 3 and 4 - As iterative processing progresses, updated CIR estimates for all users are available to the receiver after the 2nd iteration, and fully utilized by the receiver from the 3rd iteration onwards.

The following sections describe the modifications required to the various components of the receiver used during block-based processing when any of the users are mobile.

5.3.1 Successive Interference Cancellation

SIC is a sequential decoding process adopted from cellular communications [27] and designed to decode each user in succession. Along the way, previously decoded users are treated as interferers and their decoded symbols and channel estimates are combined to construct an estimate of the interference with respect to the target user. In underwater acoustics, SIC can be applied with intelligent synchronization and scaling of the constructed interference, potentially removing MAI without excessive noise enhancement.[36] Furthermore, with multiple iterations of the SIC framework, all users can benefit from interference cancellation, increasingly improving the symbol decoding and channel estimation performance for all users.

However, when any of the users are in motion, the receiver must be aware of the changes to the interference in the Doppler dimension induced by the resampling process targeted at a specific user. Because resampling is performed on the overlapping signals, what may be a Doppler correction for one user will be a

Doppler distortion for interfering users. To model the effect of resampling on the MAI, the users first are numbered by their order in the SIC process (i.e. user k is decoded immediately prior to user $k+1$). To decode user k, the receiver begins by resampling with respect to λ_k, the target user's Doppler coefficient. It can be shown that the baseband equivalent to passband resampling is

$$r_{\mathrm{pb}}(\lambda_k^{-1}t) \iff r(\lambda_k^{-1}t)e^{j2\pi f_c\left(\lambda_k^{-1}-1\right)t}, \tag{5.22}$$

which leads to the following baseband interference model

$$r_i(\lambda_k^{-1}t)e^{j2\pi f_c\left(\lambda_k^{-1}-1\right)t} = h_i^k(t) \star x_k(t-\Delta_k) + I_{i,k}^{k<l}(t) + I_{i,k}^{k>l}(t) + n_i'(t), \tag{5.23}$$

where

$$I_{i,k}^{k<l}(t) = \sum_{l<k} h_i^l(t) \star x_l\left(\frac{\lambda_l}{\lambda_k}t - \Delta_l\right) e^{j2\pi f_c\left(\frac{\lambda_l}{\lambda_k}-1\right)t} \tag{5.24}$$

is the interference from all previously decoded users,

$$I_{i,k}^{k>l}(t) = \sum_{l>k} h_i^l(t) \star x_l\left(\frac{\lambda_l}{\lambda_k}t - \Delta_l\right) e^{j2\pi f_c\left(\frac{\lambda_l}{\lambda_k}-1\right)t} \tag{5.25}$$

is the interference from all users that have yet to be decoded and $n_i'(t)$ is the resampled noise process. Note that an estimate of (5.25) cannot be formed until after the first iteration of SIC, at which point all users have been decoded at least once and estimates of $h_i^l(t)$ and $x_l(t)$ for $l > k$ are available from the previous iteration (see Fig. 2).

The SIC process individually estimates each component of the sum in (5.24) (for interferers $l < k$) and, after the first iteration, each component of the sum in (5.25) (for all interferers $l \neq k$). The interference from a user l onto user k at receiver i is constructed as

$$I_{i,k}^{l}(t) = h_i^l(t) \star x_l\left(\frac{\lambda_l}{\lambda_k}t\right) e^{j2\pi f_c\left(\frac{\lambda_l}{\lambda_k}-1\right)t} \tag{5.26}$$

from estimates of all necessary quantities. Unlike previous work on SIC, the interference estimates must be Doppler shifted by λ_l/λ_k to compensate for the effects of resampling. The interference is then scaled by $\alpha_{k,l}$ to minimize noise and error

enhancement and synchronized to the target user's signal by time delay $\Delta_{k,l}$ before being subtracted from the target signal to form

$$r_i^{(k)}(t) = r_i(\lambda_k^{-1}t)e^{j2\pi\left(\lambda_k^{-1}-1\right)t} - \sum_{l\neq k}\alpha_{k,l}I_{i,k}^{l}(t-\Delta_{k,l}), \tag{5.27}$$

the signal used to decode the k^{th} user's data by ATR and to update the receiver's estimate of $h_i^k(t)$ by MP. The specific choice of $\alpha_{k,l}$ and $\Delta_{k,l}$ is discussed in previous work and does not require adaptation for moving sources.[36] Finally, the efficiency of the SIC process is defined as

$$e_k = \frac{\sum_{i=1}^{N}\int\left|\left|r_i(\lambda_k^{-1}t)\right|\right|^2 dt}{\sum_{i=1}^{N}\int\left|\left|r_i^{(k)}(t)\right|\right|^2 dt} \tag{5.28}$$

which is the ratio of total signal energy before SIC (5.23) to the ratio of total energy after SIC (5.27). Values of $e_k > 1$ are interpreted as successful removal of interference, while values of $e_k < 1$ suggest the interference estimates in (5.26) are poorly correlated with the MAI and error propagation is present in the system.

In summary, the resampling process targeting user k compensates for the Doppler distortion caused by λ_k but also distorts the MAI in the process. SIC models the interference caused by user l at the differential Doppler coefficient λ_l/λ_k before scaling, synchronizing, and subtracting from the target signal.

5.3.2 Adaptive Time-Reversal Processing

As shown in Fig. 5.3, the post-SIC signals in (5.27) from all receivers $i = 1,\ldots,N$ are coherently combined by ATR to achieve an array gain while simultaneously suppressing any additional interference either synthetically produced from errors propagated through the SIC process or interference that previously could not be removed (i.e. components of (5.25) during the first iteration). The block diagram in Fig. 5.3 depicts the ATR processing for a target user k which is the same in structure as all time-reversal techniques.

The uniqueness of ATR is in the design of the filter weights $w_i^k(t)$, $i = 1,\ldots,N$ which is simply set to $h_i^k(t)$ in conventional time-reversal processing designed for single-user systems. This choice of $w_i^k(t)$ yields a matched filter receiver,

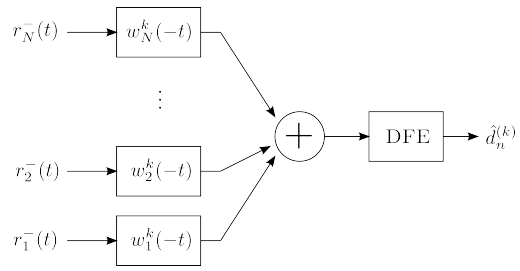

Figure 5.3: Block diagram of ATR processing targeting a user k. The filter weights are designed to balance matching the channel impulse response from user k and minimization of MAI. Following combining, a short DFE is employed to combat any residual ISI present in the effective channel.

achieving the goal of maximizing the output SNR while simultaneously suppressing intersymbol interference. With the presence of other users contributing MAI, ATR is designed instead to maximize the output signal-to-interference ratio (SINR).[2] A detailed discussion on SNR and SINR issues in time-reversal receivers is available in previous work.[36] For completeness, the ATR process is reviewed in the following discussion.

ATR first transforms the channel responses to the frequency domain

$$H_i^k(f) = \mathrm{FFT}\left\{h_i^k(t)\right\}, \tag{5.29}$$

and considers the response to all N elements array at each baseband frequency $|f| \leq \frac{W}{2}$,

$$\mathbf{d_k} = \left[\ H_1^k(f)\ H_2^k(f)\ \cdots\ H_N^k(f)\ \right]^T. \tag{5.30}$$

The filter weights in the frequency domain for the current user k are denoted $\mathbf{w}^{(k)}(f)$ and are found as the solution to the quadratic optimization problem

$$\begin{aligned} &\text{minimize} \quad \mathbf{w}^H\mathbf{R}\mathbf{w} \\ &\text{subject to} \quad \mathbf{d_k}^H\mathbf{w} = 1 \end{aligned} \tag{5.31}$$

where

$$\mathbf{R} = \sum_l \mathbf{d_l}\mathbf{d_l}^H + \sigma^2 I \tag{5.32}$$

is known a synthesized cross-spectral density matrix with regularization parameter σ^2, typically chosen as the in band noise power. Convex analysis yields the unique and optimal solution at frequency f

$$\mathbf{w}^{(k)}(f) = \frac{\mathbf{R}^{-1}\mathbf{d_k}}{\mathbf{d_k}^H\mathbf{R}^{-1}\mathbf{d_k}}. \tag{5.33}$$

These optimal solutions are transformed back into the time domain to determine the filter coefficients for user k at receiver element i,

$$w_i^k(t) = \mathrm{FFT}^{-1}\left\{\left[\ \mathbf{w}_i^{(k)}(-W/2)\ \cdots\ \mathbf{w}_i^{(k)}(W/2)\ \right]\right\} \tag{5.34}$$

for $i = 1, \ldots, N$, where $\mathbf{w}_i^{(k)}(f)$ is the i^{th} component of the vector $\mathbf{w}^{(k)}(f)$. Similar to other time-reversal processors, the effective channel at the output of the filter bank closely resembles a Dirac delta function $\delta(t)$ with a sufficient number of properly spaced receiver elements. However, a short DFE still must be employed after combining to combat the small amount of residual ISI typical of all time-reversal architectures.

In previous implementations, ATR was applied to systems limited to only stationary users (without Doppler).[38, 2] With the presence of mobile users, the Doppler effect may appear to complicate the design of ATR, but with the signal model derived in Section 5.2, ATR can be applied to systems with mobile users without modification. This is because the signal model moved the distortion caused by Doppler to the transmitted signal $x_k(t)$, removing the main source of rapid variations in $h_i^k(t, \tau)$ and allowing the channel to be modeled as block-wise time-invariant. Because ATR derives the filter bank coefficients $w_i^k(\tau)$ solely from knowledge of the channel responses $h_i^k(t)$, it does not need to be concerned with distortions of the signal $x_k(t)$ as will be confirmed in Section 5.4.

5.3.3 Matching Pursuit

Matching Pursuit is a greedy sparse channel estimation algorithm designed to estimate the nonzero portion of the CIR from largest to smallest in magnitude with repetitive projections of the transmitted signal vector onto the received vector.[35] With proper resampling, the MP algorithm can be employed without

modification for moving sources. However, as illustrated in Fig. 5.2, channel updates are not performed until the second iteration for the first decoded user since MAI estimates are not available for SIC until after the first iteration.

5.4 Experimental Results: KAM11

A data example collected from the Kauai Acomms MURI 2011 (KAM11) experiment is considered to demonstrate the receiver's feasibility in separating overlapping packets from both stationary and mobile sources. The KAM11 experiment was conducted off the west coast of Kauai in 100-m deep water. Similar to previous experiments in the area, one focus of the experiment was to investigate the impact of environmental fluctuations on acoustic communication systems in shallow water. In addition, multiuser communications was explored, particularly the impact of differential Doppler from independent sources on multiuser receivers.

5.4.1 Description of Multiuser Data

For the purposes of this study, packets collected separately during the experiment are combined in post processing to create a single packet with MAI. A two user example is considered with one stationary and one mobile user transmitting simultaneously to a vertical receiving array. Fig. 5.4 illustrates the experiment geometry, with both mobile and stationary users transmitting from positions south of the receiver. The moving source was traveling at a radial velocity of approximately 1.3 m/s with $f_d = -19$ Hz and from a distance of 1.27 km at the time of transmission (JD189 16:47) marked in Fig. 5.4 by a red circle ($\circ$). The data from the stationary source had been collected a few days earlier (JD186 03:41), and was positioned roughly 3 km away from the receiver marked by a red rectangle ($\square$). Both users transmitted a 10.5-s packet of symbols at a rate of 5 ksym/s over the 20-30 kHz band with the stationary user transmitting QPSK symbols while the mobile user transmitted BPSK symbols as indicated in Fig. 5.6. The symbols were shaped with a root-raised cosine filter with a rolloff factor of 1. Spreading codes were not used by either user (e.g. Gold or Kasami codes), and instead each user

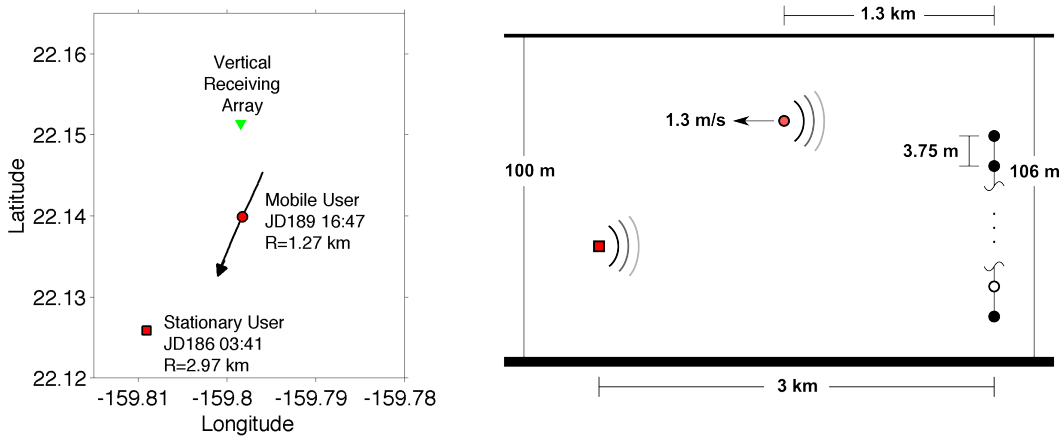

Figure 5.4: (Color online) Reconstruction of a portion of the KAM11 experiment in 100-m deep water. A moving source was towed at 35-m depth at a radial velocity of approximately 1.3 m/s (R = 1.3 km). The data example combined the moving source transmission at 1.3 km range (red circle) and the stationary source transmission at 3 km range (red square) to the receiving array. The second deepest hydrophone marked by the open circle was malfunctioning during this portion of the experiment. Data from this hydrophone was not considered in this analysis.

transmitted signals designed for single-user systems.

At the receiver, each data packet was received independently and a multiuser packet was constructed in post processing by adding the two packets together. Although the packets were roughly synchronized at the receiver by construction, the problem of truly asynchronous multiuser communications has been discussed for stationary sources[46]. The average element-level input SNR for each user was 20.1 dB and 34.0 dB for the stationary and moving sources, respectively. This large difference in received SNR introduced the near-far problem, in which one (or many) users transmit with enough power to mask the presence of users transmitting with lower power. Typically, this is addressed at the networking level with the base station requesting louder users to transmit with less power or quieter users with more. Although this problem is interesting in itself, it is beyond the scope of this paper. To compensate for the near-far problem, the received packet from the moving source was scaled down by a factor of 4 (or -12 dB) before the multiuser packet was created, which also minimized the effect of the second noise contribution from the additional packet, a consequence of creating multiuser data in post processing. The final average input SNRs experienced by each of the users in the combined multiuser packet was 19.9 dB and 21.6 dB for the stationary and moving sources, respectively. These input SNRs are only slightly lower than expected, because the noise component within the moving source data after scaling effectively is dominated by the noise within the stationary source data.

5.4.2 Analysis of Time-Varying Channel

As with all time-reversal receivers, an initial estimate of the CIR and the mean Doppler shift for each user is required to begin the processing. However, with multiple users transmitting, this estimation generally needs to performed in the presence of MAI. A short training sequence (250 symbols) at the beginning of each user's packet was used by the MP algorithm to obtain an initial estimate of each user's CIR at each receiving element after resampling (for the mobile user), and is shown in the top panels of Fig. 5.5. The horizontal axes in the CIR estimates represent the relative arrival times between the paths after the bulk travel time

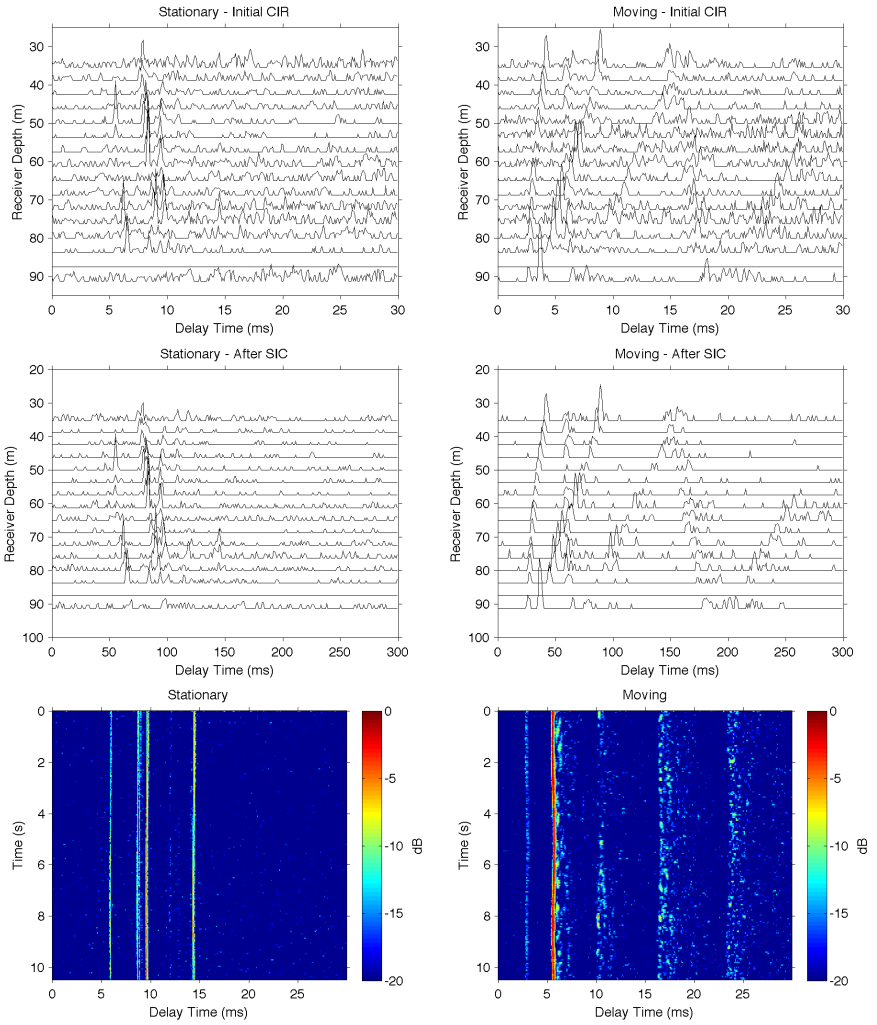

(a) (b)

Figure 5.5: (Color online) Analysis of time-varying channel for (a) stationary, and (b) moving sources after Doppler compensation: (top) initial CIRs between both sources and each array element estimated in the presence of MAI; (middle) CIR estimates between both sources and each array element estimated after MAI has been removed after multiple iterations of the SIC process; and (bottom) time-varying CIRs between both users and a single receiver element at 73-m depth estimated with the MP algorithm after interference cancellation during iterative processing.

to the receiver has been removed. Although the initial CIR estimates may appear quite poor, as the receiver updates the channel after significant amounts of MAI have been removed, they can be replaced with higher quality estimates as shown in the middle panels of Fig. 5.5. Furthermore, as the receiver tracks the time-varying CIRs for both the mobile and stationary users during block-wise processing of the resampled signal, the temporal variability of the channels can be observed by compiling these estimates in time. The time-varying CIRs plotted for each on a single receive channel at 73-m depth in the bottom panels of Fig. 5.5 illustrate the variations in the channel for both users. As expected, the mobile user experiences a CIR with much faster temporal variations than the stationary user. Note that for the mobile user, resampling has corrected the drift in arrival times of the paths.

5.4.3 Results from Iterative Decoding

Four iterations of the interference cancellation receiver discussed in Section 5.3 were applied to the multiuser data. After baseband conversion and sampling at twice the symbol rate, the received data packet was decoded in a block-by-block fashion with a block size of 50 ms or 250 symbol periods. The block length was chosen such that the distance traveled by the source over the duration of a block was roughly on the order of a wavelength.[47] From the 210 total blocks, 5 blocks (or 0.25 s) were reserved for training purposes. A large training interval was necessary mainly for two reasons. First, the initial CIR estimates were quite poor (see Fig. 5.5). Second, RLS-based equalizers were utilized with large forget factors (0.998 for both users) requiring large training intervals to achieve initial convergence. Results from decoding the remaining 205 blocks (or 10.25 s) in decision-directed mode are presented below.

After each iteration, soft symbol estimates were collected at the DFE slicer input, aggregated over all blocks, and are shown in Fig. 5.6. Fig. 5.7a illustrates the aggregate symbol error rate after each iteration. During block-wise processing, channel estimates from the final iteration of decoding the previous block were used during the first iteration of the next block. As discussed in the previous section, the mobile user's CIR varied at a much faster time scale than the stationary user,

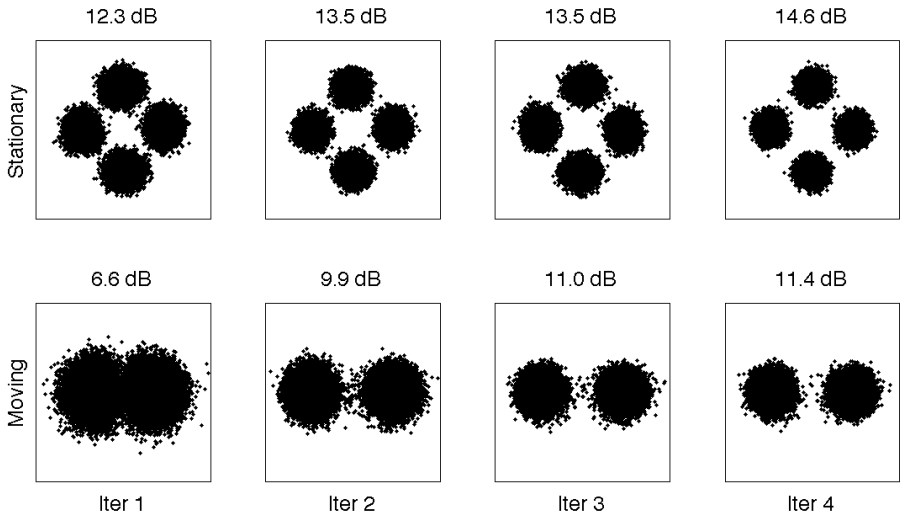

Figure 5.6: Scatter plots of soft symbol estimates of moving and stationary users after each of four iterations of the receiver. Decoded symbols are fed back to improve the interference cancellation, aiding the receiver in future processing iterations.

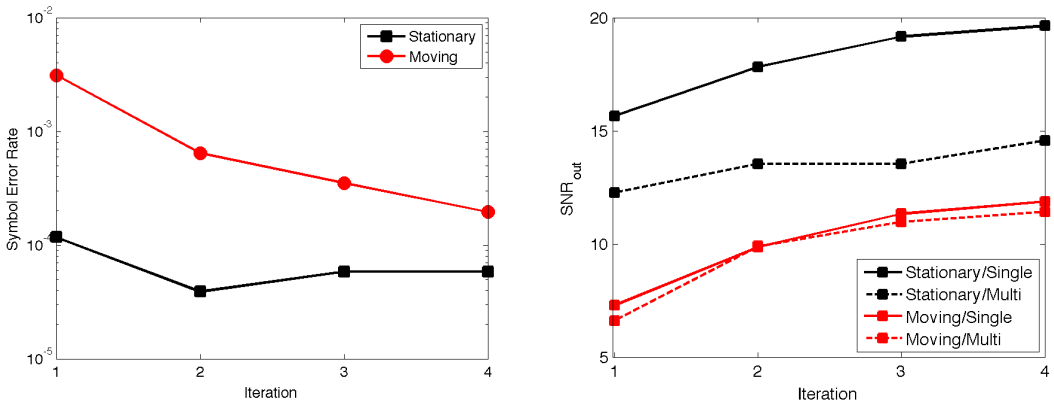

(a) (b)

Figure 5.7: (Color online) (a) Aggregate symbol error rate for each user after each iteration of the interference cancellation receiver; and (b) performance comparison between processing of the packets prior to combining with a single-user receiver (solid curves) to multiuser processing of the combined packet with the proposed multiuser receiver (dashed curves).

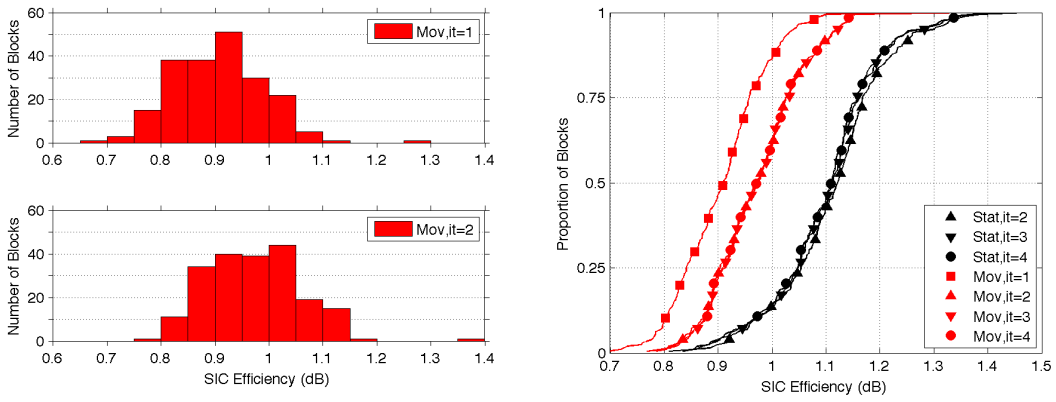

(a) (b)

Figure 5.8: (Color online) (a) Histogram of SIC efficiency for the mobile user after the first and second iterations, and (b) cumulative distribution of SIC efficiency for each user after each iteration and over all 190 decoding blocks. Positive values represent successful interference removal with 1 dB interpreted as approximately 20% of interference removed as a percentage of total signal power.

and this is evident in the 3.3 dB performance increase between iterations 1 and 2 for the mobile user. After the first iteration, a channel update could be performed for the current block, and the second iteration made use of these updated channels for the first time. The channel for the stationary user varied at a slower scale, and the channel estimates from the previous block were accurate enough to yield a high aggregate output SNR of 12.3 dB even after the first iteration.

After the first two iterations, the symbol estimates for both users were accurate enough to produce high quality channel updates and the interference cancellation process converged. The convergence of the interference cancellation process can be observed by considering the efficiency as defined in (5.28) after each iteration and is illustrated in Fig. 5.8. The efficiency was measured while decoding each block, and the distribution of the efficiency over the blocks was considered after each iteration. For example, Fig. 5.8a illustrates the histograms of SIC efficiency during the first and second iterations for the mobile user. Fig. 5.8b illustrates the distribution of SIC efficiency for both users after each iteration. The

quantiles are given by the horizontal axis value at distribution levels of 0.25, 0.5 (the median), and 0.75.

With equivalent received SNRs for both users, an efficiency of 1 dB corresponds roughly to 20% of interference removed as a percentage of total signal power. In this situation, a maximum of 50% of the total signal power can be removed which corresponds to a maximum efficiency of 3 dB. Note that the efficiency describes the performance of SIC alone, and the additional interference removed by further processing with ATR is not captured by (5.28). As shown in Fig. 5.8, the SIC process improved from iteration 1 to 2 for the mobile user, but remained largely unchanged thereafter, suggesting convergence of the interference cancellation after the 2nd iteration. For the stationary user (the first user in the decoding sequence) interference cancellation was performed for the first time during the 2nd iteration (see Fig. 5.2), after which the efficiency remained largely unchanged.

Further improvements observed in the final two iterations in Fig. 5.6 and 5.7a can be attributed to slow convergence of the DFE weights, where an RLS algorithm with forget factor of 0.998 was employed. With such a high forget factor, the RLS time constant defined by $(1-\lambda)^{-1}$,[48] was 500 symbol periods (or two block lengths), and a total of four iterations was necessary to fully converge the equalizer.

For comparison purposes, the user's packets also were decoded individually (in the absence of MAI), with a single-user receiver based on conventional time-reversal processing and MP.[21] Before decoding the packet from the mobile user, the packet was scaled by a factor of 0.25 and ambient noise was added to achieve an input SNR of roughly 21.8 dB. The single-user receiver was applied with the same block size (250 symbol periods) and the same DFE (with RLS forget factor 0.998). Again, with a large forget factor and subsequent RLS constant of two block lengths, four iterations of processing were needed to achieve tap convergence before moving on to the next block. Fig. 5.7b illustrates the output SNR after each iteration for both single and multiuser processing. The comparison provides some insight into the following limitations of the receiver:

- The performance of the single-user receiver applied to the stationary source

packet data far exceeds the performance of the multiuser receiver applied to the combined stationary and moving source packet data. As illustrated in the time-varying CIR for the moving source in Fig. 5.5, the later surface-scattered arrivals are complex and vary rapidly in time, creating ISI which sets an effective noise floor for the single-user receiver.

- Comparing the output SNRs between single-user and multiuser receivers, there is a large disparity in performance between single and multiuser decoding for the stationary source (black curves in Fig. 5.7b), while there is minimal disparity for the mobile user (red curves in Fig. 5.7b). For the stationary user, the mobile user's rapidly varying, surface-scattered arrivals act as a significant source of MAI that cannot be removed completely by this receiver leading to a large performance gap when compared to single-user decoding. This is evident when comparing the CIRs after SIC in the middle panels of Fig. 5.5. Comparing the two CIR estimates, it is apparent that SIC has removed much of the MAI from the stationary source before estimating the CIR for the moving source (middle right panel). In contrast, SIC cannot remove all of the MAI from the moving source before CIR estimation for the stationary source (middle left panel). In comparing the single-user and multiuser decoding performances for the mobile user, the residual MAI from the stationary user is masked by the residual ISI from the later surface-scattered paths, and both single and multiuser processing lead to similar results.

5.5 Summary

A receiver was developed capable of separating overlapping packets from multiple, potentially mobile, users transmitting to a shared base station. The receiver embedded an ATR processor within an iterative SIC framework, designed to decode each user in succession and form interference estimates to aid in the decoding of other users in the system. In comparison with other SIC architectures limited to systems with only stationary users, this architecture modified the SIC process to track the effects of resampling on the MAI that would have been dis-

tributed across the Doppler dimension when the users experienced different mean Doppler shifts. With multiple iterations, the receiver was shown to be capable of separating a two-user packet collected during the KAM11 experiment. A block-wise implementation allowed the receiver to track the time-varying CIRs for each user, maintaining successful decoding throughout the 10.5-s packet and converging the SIC portion of the receiver within 2 iterations.

Acknowledgements

This work was supported by the Office of Naval Research under grant N00014-07-1-0739.

Chapter 5, in full, is a reprint of the material as it appears in "Multiuser Acoustic Communications with Mobile Users, S. E. Cho, H. C. Song, and W. S. Hodgkiss, *Journal of the Acoustical Society of America*, submitted on May 29, 2012. The dissertation author was the primary investigator and author of this paper.

Chapter 6

Concluding Remarks

6.1 Summary of Dissertation

This dissertation detailed the author's research in multiuser communications in the challenging underwater acoustic environment. These channels are characterized by severe delay spread, fast variations, and Doppler effects (signal compressions and dilations) when sources are in motion. The first Chapter provided the necessary background material about the shallow water underwater acoustic channel and described the impact of the dominant characteristics of this environment on popular MAC system designs. The remaining chapters discussed a multiuser receiver design based on a combination of TR combining and SIC. Each chapter modified and applied the receiver to successively more general channels, providing examples on data collected during at-sea experiments with each design. Table 6.1 summarizes the results from experimental data discussed throughout the dissertation. Note that data rates and spectral efficiencies do not account for overhead from training, and in Chapter 4, the data rate quoted is the maximum data rate, the period when the users were overlapping in time.

The first approach (Chapter 2) introduced SIC for UWAC and embedded a conventional TR combiner within the iterative interference cancellation framework. The CIRs between the users and each receiver were assumed to be time-invariant, which coincides with the most benign channels encountered in this environment. SIC combined estimates of the cross q-functions formed from prior knowledge of

Table 6.1: Summary of Experimental Results

Chapter	Experiment	N_{users}	Data Rate (kbps)	Spec. Eff. (b/s/Hz)
2	FAF-05	3	6	6
	FAF-06	2	24	2
3	KAM11	2	25	2.5
4	KAM11	2	35	3.5
5	KAM11	2	15	1.5

the channel and prior decoded symbols to estimate and remove MAI, steadily improving the decoding performance through multiple iterative applications. The second receiver (Chapter 3) discussed a receiver capable of separating stationary users transmitting through a time-varying channel. This receiver combined the SIC procedure with ATR to provide additional MAI suppression. Here, SIC was performed at the multichannel level (before the multichannel combiner) and was shown to be able to provide the MP channel estimation algorithm with interference mitigated signals. These signals were combined with ATR, a TR combiner with additional MAI suppressing capabilities. Data from the KAM11 experiment confirmed the receiver's operability in time-varying environments and higher frequency bands (20-30 kHz). Chapter 4 discussed the applicability of the previous SIC, ATR, and MP receiver in asynchronous communications environments. Without a feedback channel, the users' packets could not be assumed synchronized at the receiver, and a method for estimation of the users' initial CIRs in the presence of strong MAI was considered. Finally, in Chapter 5, the receiver was modified to be able to separate multiuser transmissions when any of the users potentially were in motion. The Doppler effect was introduced into the system model and was addressed via resampling of the received waveform. However, since not all the users would experience the same Doppler distortion, the interference model also was modified to incorporate the effects of Doppler both before and after resampling, and the SIC process was modified to remove interference at differential Doppler shifts. Moving source data from the KAM11 experiment were used to illustrate the capability of the receiver in this general shallow water environment.

The major contributions of this dissertation are summarized as follows:

- Analysis of experimental data was a point of emphasis throughout the research efforts. This dissertation provided analysis from three experiments conducted at sea (FAF-05, FAF-06, and KAM11).

- A framework for interference cancellation was introduced capable of separating transmissions from multiple, possibly mobile, users in a time-varying shallow water environment. With iterative processing, this receiver achieved the goal of providing multiple users with individual channels by removing interference from competing users.

- Multiple-access communications was achieved with high spectral efficiencies, increasing the total throughput over a single user system linearly with the number of users. Other division schemes (e.g. TDMA, FDMA, and CDMA) typically require a throughput loss to guarantee MAI-free systems. The systems discussed throughout this dissertation utilized SDMA, leveraging the complexities of the underwater acoustic channel to separate the users at the receiver.

- The receivers discussed throughout the dissertation required no feedback from the receiver. The common receiver was capable of separating overlapping packets without relaying information back to competing users in the system. From a networking perspective, this was highly desirable, as the overhead required for a feedback channel in the shallow underwater acoustic environment could be avoided.

- The latter designs were shown to be capable of tracking the time-varying CIRs from multiple users in the presence of strong MAI. All of the designs required accurate knowledge of the CIR between the user and each element of the receiving array, and accurate updates of the CIR throughout the decoding process were critical to the receiver designs throughout this dissertation. The channel also was modeled as sparse, allowing the receiver to obtain high quality estimates with fewer data observations. Sparse channel estimation also eliminated the performance loss from using irrelevant but nonzero values in the CIR estimates.

- With users potentially in motion, the issue of decoding packets distorted by different Doppler shifts was addressed. MAI was tracked through the resampling process targeted at a single user and was removed successfully with a modified SIC algorithm.

6.2 Topics for Further Investigation

Multiuser underwater acoustic communications is a relatively unexplored area of research. As such, many extensions of this research as well as new investigations into MAC are possible. Some of them are listed below.

- The adaptive receivers presented in this dissertation were capable of tracking a changing CIR by applying the MP algorithm in a block-by-block fashion. However, the receivers discussed throughout the dissertation did not consider the previous estimates of the CIR, which can be informative if the channel is not fading too rapidly, and the block size is chosen appropriately. An adaptive MP algorithm that is capable of utilizing an outdated but informative estimate would be beneficial to these receivers [49, 50].

- An important point of focus for all multiple-access systems is the challenge of overcoming the near-far problem. The near-far problem exists when there is a large discrepancy in the received SNR two or more users. This situation can arise if a user is transmitting with more power than another or if one user is simply much closer to the receiver than the others. Although touched upon in this dissertation, most of the analyzed data exhibited users with comparable received SNR, and extreme cases of the near-far problem were left unaddressed.

- Although maximizing throughput with SDMA was a focus of this dissertation, the robustness of these receivers was for the most part left for further exploration. Although they would reduce the total throughput, the addition of error correction codes certainly would enhance the robustness of these receivers, and their introduction is certainly a topic of further exploration.

- Another possible avenue to increase the robustness of these systems is to allow the users to employ short spreading codes to achieve a coding gain. Although this also would result in throughput loss, the techniques discussed throughout this dissertation would still apply, allowing shorter codes to be employed than otherwise possible. The combination of SIC and CDMA potentially would be more desirable in more challenging environments (i.e. the near-far problem).

- The systems studied in this dissertation were constructed with a small number of users (2 or 3). In much larger systems, e.g. sensor networks, the applicability of these receivers should be investigated further. Although the concepts of interference cancellation still would apply to systems with larger numbers of users, the other aspects of the system (e.g. initial frame synchronization and channel acquisition) may become challenging in these situations.

- In the data considered for this dissertation, each of the users transmitted single-carrier, wideband signals to a common base station. However, one of the benefits of SIC is that each user's signal is decoded individually. Although the receiver would be more complicated, it would be feasible to allow users to employ different transmission schemes such as OFDM while other users transmitted single-carrier signals.

- If all users were limited to orthogonal frequency division multiplexing (OFDM), orthogonal frequency division multiple access (OFDMA) could also be explored. Doppler distorted MAI from competing users in motion would introduce multiple-access, inter-carrier interference (ICI) that would need to be addressed. Interference potentially could be modeled and removed within each OFDM bin with the SIC process. This potentially could simplify the overall SIC decoding structure over single-carrier systems with large amounts of ISI.

- All of the users in this dissertation were restricted to single transmitters. More generally, these users could in fact each utilize multiple transmitters to increase the throughput or robustness of the system. How best to utilize these additional resources would be an interesting point of further exploration.

Bibliography

[1] M. Stojanovic and Z. Zvonar, "Multichannel processing of broadband multiuser communication signals in shallow water acoustic channels," *IEEE J. Ocean. Eng.*, vol. 21, pp. 156–166, 1996.

[2] H. C. Song, J. S. Kim, W. S. Hodgkiss, W. Kuperman, and M. Stevenson, "High-rate multiuser communications in shallow water," *J. Acoust. Soc. Am.*, vol. 128, no. 5, pp. 2920–2925, 2010.

[3] N. Fair, A. Chave, L. Freitag, J. Preisig, S. White, D. Yoerger, and F. Sonnichsen, "Optical modem technology for seafloor observatories," in *Proc. MTS/IEEE OCEANS'06*, pp. 1–6, 2006.

[4] H. C. Song, W. A. Kuperman, and W. S. Hodgkiss, "Basin-scale time reversal communications," *J. Acoust. Soc. Am.*, vol. 125, no. 1, pp. 212–217, 2009.

[5] H. C. Song, S. Cho, T. Kang, W. S. Hodgkiss, and J. R. Preston, "Long-range acoustic communication in deep water using a towed array," *J. Acoust. Soc. Am.*, vol. 129, no. 3, pp. EL71–EL75, 2011.

[6] D. Kilfoyle and A. Baggeroer, "The state of the art in underwater acoustic telemetry," *IEEE J. Oceanic Eng.*, vol. 25, no. 1, pp. 4–27, 2000.

[7] J. Catipovic, "Performance limitations in underwater acoustic telemetry," *IEEE J. Oceanic Eng.*, vol. 15, no. 3, pp. 205–216, 1990.

[8] F. B. Jensen, W. A. Kuperman, M. B. Porter, and H. Schmidt, *Computational Ocean Acoustics*. New York: AIP Press, 1994.

[9] J. Proakis, *Digital Communications*. New York: McGraw-Hill, 2001.

[10] E. Sozer, M. Stojanovic, and J. Proakis, "Underwater acoustic networks," *IEEE J. Ocean. Eng.*, vol. 25, no. 1, pp. 72–83, 2000.

[11] M. Stojanovic, J. Proakis, J. Rice, and M. Green, "Spread spectrum underwater acoustic telemetry," in *Proc. MTS/IEEE OCEANS'98*, vol. 2, pp. 650–654, 1998.

[12] L. Freitag, M. Stojanovic, S. Singh, and M. Johnson, "Analysis of channel effects on direct-sequence and frequency-hopped spread-spectrum acoustic communication," *IEEE J. Oceanic Eng.*, vol. 26, no. 4, pp. 586–593, 2001.

[13] P. Hursky, M. B. Porter, and M. Siderius, "Point-to-point underwater acoustic communications using spread-spectrum passive phase conjugation," *J. Acoust. Soc. Am.*, vol. 1280, no. 1, pp. 247–257, 2006.

[14] T. C. Yang and W.-B. Yang, "Performance analysis of direct-sequence spread-spectrum underwater acoustic communications with low signal-to-noise-ratio input signals," *J. Acoust. Soc. Am.*, vol. 123, no. 2, pp. 842–855, 2008.

[15] M. Stojanovic and L. Freitag, "Multichannel detection for wideband underwater acoustic CDMA communications," *IEEE J. Ocean. Eng.*, vol. 31, no. 3, pp. 685–695, 2006.

[16] T. C. Yang and W. Yang, "Interference suppression for code-division multiple-access communications in an underwater acoustic channel," *J. Acoust. Soc. Am.*, vol. 126, pp. 220–228, 2009.

[17] M. Stojanovic, J. A. Capitovic, and J. G. Proakis, "Phase-coherent digital communications for underwater acoustic channels," *IEEE J. Ocean. Eng.*, vol. 19, pp. 110–111, 1994.

[18] M. Stojanovic, J. A. Capitovic, and J. G. Proakis, "Adaptive multi-channel combining and equalization for underwater acoustic communictions," *J. Acoust. Soc. Am.*, vol. 94, pp. 1621–1631, 1993.

[19] M. Stojanovic, L. Freitag, and M. Johnson, "Channel-estimation-based adaptive equalization of underwater acoustic signals," in *Proc. MTS/IEEE OCEANS'99*, vol. 2, pp. 590–595, 1999.

[20] D. Rouseff, D. Jackson, W. Fox, C. Jones, J. Ritcey, and D. Dowling, "Underwater acoustic communications by passive-phase conjugation: Theory and experimental results," *IEEE J. Oceanic Eng.*, vol. 26, pp. 821–831, 2001.

[21] H. C. Song, "Time reversal communication in a time-varying sparse channel," *J. Acoust. Soc. Am.*, vol. 130, no. 4, pp. EL161–EL166, 2011.

[22] H. C. Song, P. Roux, W. S. Hodgkiss, W. A. Kuperman, T. Akal, and M. Stevenson, "Multiple-input-multiple-output coherent time reversal communications in a shallow-water acoustic channel," *IEEE J. Oceanic Eng.*, vol. 31, pp. 170–178, 2006.

[23] H. C. Song, W. S. Hodgkiss, W. A. Kuperman, T. Akal, and M. Stevenson, "Multiuser communications using passive time reversal," *IEEE J. Oceanic Eng.*, vol. 32, pp. 915–926, 2007.

[24] A. Song, M. Badiey, V. McDonald, and T. Yang, "Time reversal receivers for high data rate acoustic multiple-input multiple-output communication," *IEEE J. Oceanic Eng.*, vol. 36, no. 4, pp. 525–538, 2011.

[25] H. C. Song, J. S. Kim, W. S. Hodgkiss, and J. H. Joo, "Crosstalk mitigation using adaptive time reversal," *J. Acoust. Soc. Am.*, vol. 127, no. 2, pp. EL19–EL22, 2010.

[26] S. Roy, T. Duman, V. McDonald, and J. Proakis, "High-rate communication for underwater acoustic channels using multiple transmitters and space-time coding: Receiver structures and experimental results," *IEEE J. Ocean. Eng.*, vol. 32, pp. 663–688, 2007.

[27] J. Andrews, "Interference cancellation for cellular systems: a contemporary overview," *IEEE Wireless Comm.*, vol. 2, pp. 19–29, 2005.

[28] T. C. Yang, "Correlation-based decision-feedback equalizer for underwater acoustic communications," *IEEE J. Ocean. Eng.*, vol. 30, pp. 865–880, 2005.

[29] H. C. Song and S. M. Kim, "Retrofocusing techniques in a waveguide for acoustic communications (l)," *J. Acoust. Soc. Am.*, vol. 121, pp. 3277–3279, 2007.

[30] H. C. Song, W. S. Hodgkiss, W. A. Kuperman, W. Higley, K. Raghukumar, T. Akal, and M. Stevenson, "Spatial diversity in passive time reversal communications," *J. Acoust. Soc. Am.*, vol. 120, pp. 2067–2076, 2006.

[31] D. Tse and P. Viswanath, *Fundamentals of wireless communication*. New York: Cambridge University Press, 2001.

[32] N. Xiang and S. Li, "A pseudo-inverse algorithm for simultaneous measurements using multiple acoustical sources," *J. Acoust. Soc. Am.*, vol. 121, pp. 1299–1302, 2007.

[33] H. C. Song, W. S. Hodgkiss, and W. A. Kuperman, "High-frequency acoustic communications achieving high bandwidth efficiency," *J. Acoust. Soc. Am.*, vol. 126, no. 2, pp. 561–563, 2009.

[34] A. Song, M. Badiey, A. Newhall, J. Lynch, H. DeFerrari, and B. Katsnelson, "Passive time reversal acoustic communications through shallow-water internal waves," *IEEE J. Oceanic Eng.*, vol. 35, no. 4, pp. 756–765, 2010.

[35] S. Cotter and B. Rao, "Sparse channel estimation via matching pursuit with application to equalization," *IEEE Trans. on Comm.*, vol. 50, no. 3, pp. 374 –377, 2002.

[36] S. Cho, H. Song, and W. Hodgkiss, "Successive interference cancellation for underwater acoustic communications," *IEEE J. Oceanic Eng.*, vol. 36, no. 4, pp. 490–501, 2011.

[37] J. Tropp and A. Gilbert, "Signal recovery from random measurements via orthogonal matching pursuit," *IEEE Trans. Inf. Theory*, vol. 53, no. 12, pp. 4655–4666, 2007.

[38] S. Cho, H. Song, and W. Hodgkiss, "Multiuser interference cancellation in time-varying channels," *J. Acoust. Soc. Am.*, vol. 131, no. 2, pp. EL163–EL169, 2012.

[39] J. Cui, J. Kong, M. Gerla, and S. Zhou, "The challenges of building mobile underwater wireless networks for aquatic applications," *IEEE Network*, vol. 20, no. 3, pp. 12–18, 2006.

[40] J. Tao, Y. Zheng, C. Xiao, and T. Yang, "Robust MIMO underwater acoustic communications using turbo block decision-feedback equalization," *IEEE J. Ocean. Eng.*, vol. 35, no. 4, pp. 948–960, 2010.

[41] J. Zhang and Y. Zheng, "Frequency-domain turbo equalization with soft successive interference cancellation for single carrier MIMO underwater acoustic communications," *Wireless Communications, IEEE Transactions on*, vol. 10, no. 9, pp. 2872–2882, 2011.

[42] C. R. Berger, S. Zhou, J. C. Preisig, and P. Willet, "Sparse channel estimation for multicarrier underwater acoustic communication: from subspace methods to compressed sensing," *IEEE Trans. on Signal Proc.*, vol. 58, no. 3, pp. 1708–1721, 2010.

[43] N. F. Josso and C. Gervaise, "Source motion detection, estimation, and compensation for underwater acoustics inversion by wideband ambiguity lag-doppler filtering," *J. Acoust. Soc. Am.*, vol. 128, no. 6, pp. 3416–3425, 2010.

[44] X. Jiang, W.-J. Zeng, and X.-L. Li, "Time delay and doppler estimation for wideband acoustic signals in multipath environments," *J. Acoust. Soc. Am.*, vol. 130, no. 2, pp. 850–857, 2011.

[45] A. Song and M. Badiey, "Time reversal multiple-input/multiple-output acoustic communication enhanced by parallel interference cancellation," *J. Acoust. Soc. Am.*, vol. 131, no. 1, pp. 281–291, 2012.

[46] S. Cho, H. Song, and W. Hodgkiss, "Asynchronous multiuser underwater acoustic communications(l)," *J. Acoust. Soc. Am.*, 2012. in press.

[47] H. C. Song, "Performance bounds for passively locating a moving source of a known frequency in oceanic waveguide using a vertical array," *IEEE J. Ocean. Eng.*, vol. 18, no. 3, pp. 189–198, 1993.

[48] D. G. Manolakis, V. K. Ingle, and S. M. Kogon, *Statistical and Adaptive Signal Processing*. New York: McGraw-Hill, 2005.

[49] S. Cotter and B. Rao, "The adaptive matching pursuit algorithm for estimation and equalization of sparse time-varying channels," in *Proc. 34th Asilomar Conf. Signals Syst. Comput.*, vol. 2, pp. 1772–1776, 2000.

[50] V. Stankovic, L. Stankovic, and S. Cheng, "Compressive image sampling with side information," in *Proc. 16th IEEE Image Proc. Conf. (ICIP)*, pp. 3037 –3040, 2009.